Biological Applications of Rare-Earth Based Nanoparticles

Cedric Bouzigues,[†,*] Thierry Gacoin,[‡] and Antigoni Alexandrou[†]

[†]Laboratoire d'Optique et Biosciences, Ecole Polytechnique, CNRS UMR7645 INSERM U696, 91128 Palaiseau Cedex, France and
[‡]Laboratoire de Physique de la Matière Condensée, Ecole Polytechnique, CNRS UMR7643 911128 Palaiseau Cedex, France

ABSTRACT Biomedicine and cell and molecular biology require powerful imaging techniques of the single molecule scale to the whole organism, either for fundamental science or diagnosis. These applications are however often limited by the optical properties of the available probes. Moreover, in cell biology, the measurement of the cell response with spatial and temporal resolution is a central instrumental problem. This has been one of the main motivations for the development of new probes and imaging techniques either for biomolecule labeling or detection of an intracellular signaling species. The weak photostability of genetically encoded probes or organic dyes has motivated the interest for different types of nanoparticles for imaging such as quantum dots, nanodiamonds, dye-doped silica particles, or metallic nanoparticles. One of the most active fields of research in the past decade has thus been the development of rare-earth based nanoparticles, whose optical properties and low cytotoxicity are promising for biological applications. Attractive properties of rare-earth based nanoparticles include high photostability, absence of blinking, extremely narrow emission lines, large Stokes shifts, long lifetimes that can be exploited for retarded detection schemes, and facile functionalization strategies. The use of specific ions in their compositions can be moreover exploited for oxidant detection or for implementing potent contrast agents for magnetic resonance imaging. In this review, we present these different applications of rare-earth nanoparticles for biomolecule detection and imaging *in vitro*, in living cells or in small animals. We highlight how chemical composition tuning and surface functionalization lead to specific properties, which can be used for different imaging modalities. We discuss their performances for imaging in comparison with other probes and to what extent they could constitute a central tool in the future of molecular and cell biology.

KEYWORDS: rare-earth nanoparticles · surface functionalization · biomolecule detection · chemical composition tuning · lanthanide

Detection of biomolecules is essential for many applications in biomedicine cell and molecular biology, *in vitro* or in living cells and organisms. Efficient analytical methods, such as immunassays or DNA microarrays, and imaging techniques have thus been developed for decades. These applications are however often constrained by the available probes, whose optical properties may limit the imaging possibilities. The development of probes for labeling or enhancing the efficiency of detection has thus become essential in order to improve sensitivity of analytical devices. Moreover, in cell biology, the measurement of the cell response with spatial and temporal resolution is a central instrumental problem. These issues have motivated the development of single biomolecule—such as lipids or membrane receptors—labeling and tracking in living cells or indicators of intracellular signaling species, such as calcium ions[1] or reactive oxygen species (ROS).[2]

The weak photostability of genetically encoded probes such as green fluorescent protein (GFP) or organic dyes, used for protein labeling, have however limited their biological applications. For example, the tracking of membrane proteins labeled with organic dyes can provide the measurement of membrane protein diffusion coefficients but no information on the evolution of their organization. This is due to photobleaching that occurs within a few seconds under standard conditions of illumination for single molecule detection. The use of semiconductor fluorescent nanocrystals, or quantum dots, has notably extended the scope of possible biological applications of fluorescent probes, due to their high quantum yield and high photostability.[3,4] Quantum dots have thus, for example, been used for *in vitro* assays, single protein labeling and tracking in living cells,[5,6] or imaging in small animals. However, intermittency of their fluorescence, the so-called blinking, potential cytotoxicity *in vivo,* and complex functionalization strategies[3,4,7,8] have limited their use.

These elements justify the interest for different types of nanoparticles for imaging or for protein and nucleic acid detection, such as nanodiamonds,[9−11] dye-doped silica particles,[12,13] or metallic nanoparticles.[14,15] One of the most active fields of research in the past decade has thus been the development of rare-earth doped nanoparticles, whose optical properties and low cytotoxicity are promising for biological applications.[16−19] Attractive properties of rare-earth doped

* Address correspondence to cedric.bouzigues@polytechnique.edu.

Received for review June 28, 2011 and accepted October 7, 2011.

Published online October 08, 2011
10.1021/nn202378b

nanoparticles include high photostability, absence of blinking, extremely narrow emission lines, large Stokes shifts, long lifetimes that can be exploited for retarded detection (consisting in luminescence detection taking place after the excitation has stopped and after short-lived, approximately nanosecond, fluorescence has decayed), and facile functionalization strategies when synthesized in water. Moreover, unique, reversible oxidoreduction processes of the rare-earth ions can be exploited for oxidant detection, and the high magnetic moment of certain ions, like Gd^{3+}, under magnetic field renders them potent contrast agents for magnetic resonance imaging.

In this review, we present different applications of rare-earth based nanoparticles for biomolecule detection and imaging *in vitro*, in living cells or in small animals. We will here focus mainly on rare-earth doped nanoparticles, which may harbor thousands of ions. Extensive efforts have also been dedicated to rare-earth ion chelates or organic complexes involving one or a limited amount of ions[20] and have managed to exploit several of the unique rare-earth ion properties.[21−23] Nanoparticles, however, present the additional advantage of single-particle detection due to the large number of ions present and the absence of blinking renders them competitive with respect to quantum dots for single biomolecule tracking. Furthermore, the nanoparticle surface can be seen as a platform where multiple functionalization and targeting groups can be easily grafted.

PREPARATION OF RARE-EARTH-BASED NANOPARTICLES

Synthesis. Elaboration of rare-earth doped nanoparticles has been the subject of an increasing number of publications since about 2000.[24,25] Studies usually concern compositions that are already well-known to be highly efficient in the bulk state and developed mainly for lighting and display applications.[26] Other compositions have also been studied to take advantage of some of the original spectroscopic properties of rare-earth ions such as upconversion, quantum cutting, persistent luminescence, *etc*.

Most compounds usually consist of a host oxide matrix-containing species that acts as light absorber (sensitizer) and the rare-earth light-emitting ions (the activator). In some cases, such as in upconversion systems, a low phonon−energy matrix may be important, which leads to a preference for fluorides rather than oxides. The intrinsic nature of the rare earth mainly determines the spectroscopic properties of the material (in terms of absorption and emission wavelength and transition efficiencies). Exceptions are found in some cases when, instead of f−f electron configuration transitions, d electrons are involved in the absorption or emission transitions, for example, in the case of Eu^{2+} and Ce^{3+}. In these cases, large absorption cross sections are observed so that these ions may be used as sensitizers, with spectroscopic properties that may be drastically affected by the host matrix through crystal field splitting.

VOCABULARY: surface functionalization – a way to introduce chemical functional groups to a surface. Materials with functional groups on their surfaces can be designed from substrates with standard bulk material properties • **Stoke's shift** – the difference (in wavelength or frequency units) between positions of the band maxima of the absorption and emission spectra (fluorescence and Raman being two examples) of the same electronic transition.

As compared to quantum dots, a major difference is expected in rare-earth compounds considering that the states involved in the transitions are mainly localized within the sensitizer and activator species, while energy transfer processes occur through dipolar or exchange interactions. The consequence is that these systems are not expected to exhibit quantum confinement effects, at least for sizes of more than one or two nanometers. This means that the exact control of size distribution is not as critical as for quantum dots. On the other hand, homogeneous dispersion and optimum concentration of activator/sensitizer ions is of crucial importance due to concentration quenching effects. Rare-earth distribution within the host matrix, in addition to the appropriate control of their oxidation state, is thus a critical issue to be addressed when considering synthesis of nanoparticles.

Different processes may be used for the elaboration of nanoparticles in the objective of providing well-dispersed suspensions. Processes such as laser ablation[27] and dispersion from calcinated powders[28] would in principle allow access to almost any compound known in the bulk state, but they do not yet allow a satisfying control of size and dispersion. The colloid chemistry route thus still remains the best approach. The basic principle relies on the reaction between precursors in solution, either through coprecipitation or thermal decomposition. The critical issue is the ability to obtain particles with sufficient crystallinity, despite the low temperatures involved in these soft chemistry routes as compared to bulk material synthesis, performed at high temperatures (typically 900−1400 °C) from solid state reactions. This aspect is probably the main reason for the limited number of compounds that have been investigated up to now, as compared to the numerous known bulk compositions. This also explains why initial investigations were achieved on compounds such as YVO_4 and $LaPO_4$ compositions.[24,25,29,30] These materials, which are efficient phosphors in the bulk state, can indeed be obtained with a reasonable crystallinity from simple

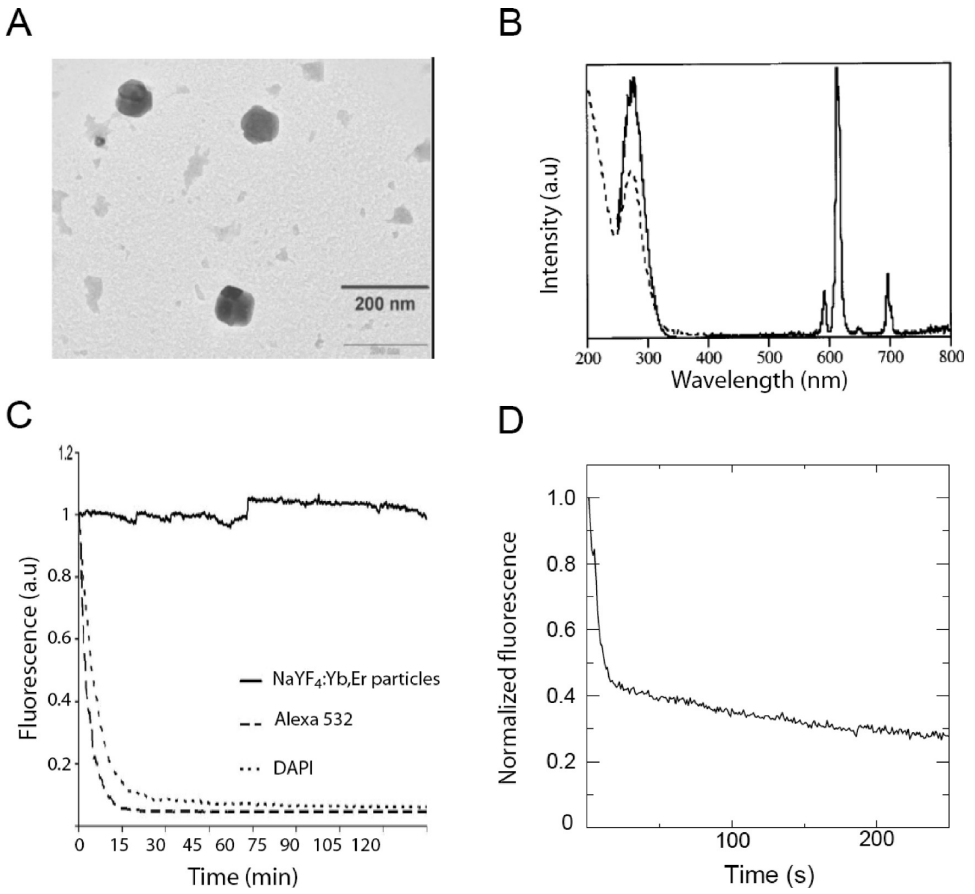

Figure 1. (A) Transmission electron microscope image of Gd_2O_3:Eu nanoparticles. Reprinted with permission from ref 75. Copyright 2005 SPIE. (B) Absorption (dashed line), luminescence excitation (for emission at 615 nm) and emission (excitation at 280 nm) spectra (solid lines) for a YVO_4:Eu nanoparticle colloidal solution. Reprinted from ref 25. Copyright 2000 American Chemical Society. (C) Luminescence evolution for NaYF4:Yb,Er particles under 500 mW illumination in a scanning confocal microscope. Reprinted with permission from ref 76. Copyright 2009 Elsevier. The nanoparticle luminescence level is stable under excitation in contrast to that of organic fluorophores (DAPI or Alexa532). (D) Luminescence evolution for a single YVO_4:Eu particle under continuous 1.6 kW/cm^2 illumination. Reprinted with permission from ref 77. Copyright 2009 Nature. The luminescence decay under illumination is due to photoreduction and is reversible (see section on oxidant nanoprobes).

precursor salts in water. They also accept a homogeneous incorporation of many rare-earth dopants.

Nevertheless, recent improvements in colloid chemistry have allowed the investigation of other systems through the use of hydrothermal and solvothermal processes.[16,31] As compared to conventional coprecipitation routes, reactions are achieved within high boiling point coordinating solvents at high temperature (typically 120−350 °C). This allows a good control of nucleation/growth processes, leading to particles with an excellent crystallinity and a narrow size distribution. In the case of rare-earth-doped compounds, such techniques are still limited to a few compounds (phosphates, fluorides), but extension to many other systems can surely be expected in a near future.

Among the reported rare-earth doped nanoparticles, many have already been tested for biological applications. The choice of matrix and rare-earth ion determines the chemical, magnetic, and/or spectral properties of each type of nanoparticle and renders them suitable for a specific application. Among the proposed materials, we can cite without being exhaustive: europium-doped yttrium vanadate,[24,25,30,32] or gadolinium oxide,[33] cerium- and terbium- doped lanthanum fluoride,[34] upconversion particles like erbium- and ytterbium-doped yttrium oxide,[35] yttrium oxysulfide,[36] lanthanum molybdate,[37] sodium and yttrium fluoride[38−40] or yttrium vanadate,[41] persistent luminescence particles like europium−dysprosium-manganese doped magnesium silicate.[42]

Most syntheses provide particles in the 3−15 nm or in the 20−50 nm size range (Figure 1A). The difference mainly originates from the preparation protocol (for example, solvent used for the synthesis and/or presence of complexing agents) and the corresponding control of nucleation/growth processes. This size consideration is of high importance regarding (i) the number of emitted photons per particle, which scales as the third power of their diameter and (ii) limiting processes that alter quantum efficiency. Smaller particles are indeed clearly limited by surface quenching,[43] while emission from particles in the

20−50 nm range appears to be limited mainly by the particle crystallinity.[41]

Rare-earth compounds can also be used as a doping agent in different types of nanoparticles, such as silica particles[44−47] or polystyrene beads. The objective of this approach is to use the high biocompatibility of these materials, while taking advantage of the chemical properties introduced by the rare-earth compounds. Silica nanoparticles can be produced by incorporating rare earths in the silica framework,[44,45,48] by designing core−shell (SiO_2-rare earth) particles[48,49] or by the embedding or coating of rare-earth chelates.[50,51] Silica particles are usually prepared by microemulsion methods[44,45,48,50] with lanthanides added to the reaction mix or by sol−gel processes.[47] Polystyrene−acrylic acid particles have also been dyed by rare-earth chelates[52−54] and are commercially available.

Functionalization. For the biological applications, surface functionnalization of the particles is a crucial step. The objective is first to ensure good dispersion of the particles in biological media, that is, in water at neutral pH and high ionic strength. Second, particles should bare specific organic or bio-organic groups which aim at targeting specific receptor sites, and/or ensuring inocuity in the case of *in vivo* experiments.

Immediately after synthesis, particles usually have a specific surface chemistry required to control the nucleation/growth process and appropriate dispersion in the solvent used. Biological applications thus require a step of postsynthesis functionalization. Strategies may be common to those used for other types of particles such as metallic particles or quantum dots.[3,4,55] However, surface derivatization of particles synthesized in water is clearly more straightforward[56,57] as compared to that of particles, such as semiconductor quantum dots, synthesized in organic solvents which require a hydrophobic to hydrophilic adaptation by elaborate chemical methods.[3,4,7,8] Usually, hydrophobic nanoparticles are first coated to ensure their stability in aqueous medium, by ligand exchange[58,59] and/or silica[32,58] or polymer coating.[8,60]

Functionalization strategies consist of a first step which aims at covering the surface of the particles with reactive groups (amino, carboxylates, thiols, aldehydes, *etc.*) so as to ensure, in a second step, the further coupling of biomolecules of interest such as streptavidin or antibodies. Different methods can be used for the first step, such as direct surface grafting of molecules or encapsulation with a polymer[61] or with a thin shell of organosilane carrying amine or other functional groups.[32,36,38,56,57] In the case of oxide nanoparticles, silica and organosilane coating is quite staightforward because of the presence of surface hydroxyle groups that act as a coupling agent with silanes. For *in vivo* applications, as in the case of other types of nanoparticles, to ensure furtivity in the blood circulation and avoid detection by the immune system, the nanoparticles are typically coated with poly(ethylene glycol) (PEG)[62,63] or Dextran molecules.[64,65]

PROPERTIES OF RARE-EARTH DOPED NANOPARTICLES

Optical Properties. The optical properties of rare-earth-doped nanoparticles are determined by the chemical nature of their constituents (doping ions and matrix). Their luminescence is in most cases due to forbidden transitions among different f-electron configurations of the rare-earth ion (except for Ce^{3+} and Eu^{2+} involving d-electrons). These low-lying energy levels are well isolated from the environment, and therefore the transition energy varies little with the host material and the nanoparticle size. As a consequence, absorption (typically 1−5 nm broad)[25,29] and emission peaks (typically 10 nm broad)[25,29,34] are both narrow compared to organic dyes or quantum dots (Figure 1B).

The nanoparticles can be either excited using a transition of the matrix (usually in the UV) and subsequent energy transfer to the rare-earth ion or using direct excitation of the rare-earth ion directly responsible for the emission or able to transfer its energy to the emitting ions, in the case of codoping such as Ce−Tb. In most of the cases, a large Stokes shift is involved (∼150 nm for YVO_4:Eu nanoparticles), much larger than typical Stokes shifts of organic fluorophores, which further facilitates background elimination. UV excitation is not optimal for applications in living cells or organisms and, therefore, direct excitation of, for instance, Eu^{3+} has been employed using an argon laser and has allowed single-particle detection.[32] In this case, the narrowness of the absorption lines limits the usable light sources for imaging. However, the continuous development of compact, high-power, inexpensive solid-state lasers and light-emitting diodes should provide alternative solutions.[66]

Upconversion particles provide a highly efficient strategy for background signal elimination since they absorb two or more photons to emit photons of higher energy.[67,68] Thus, the nanoparticle emission is anti-Stokes shifted and takes place in a wavelength range where endogenous biomolecule emission is absent. In addition, upconversion nanoparticles are excited in the near-infrared allowing deeper tissue penetration. The upconversion from the near-infrared to the visible takes place *via* energy transfer between different dopant ions and/or excited-state absorption, and single particle imaging has been recently demonstrated.[40,63,69] Because these upconversion processes involve real long-lived metastable states with lifetimes on the microsecond scale, inexpensive continuous-wave lasers can be used, whereas multiphoton excitation typically requires expensive, pulsed lasers. Biomedical applications using upconversion nanoparticles have been demonstrated for erbium- and ytterbium-doped

TABLE 1. Optical Properties of Different Probes[a]

emitter	cross-section (cm^2)	extinction coefficient ($M^{-1}\cdot cm^{-1}$)	quantum yield	photon emission rate (s^{-1})	emission width (nm)	time before photobleaching (s)	lifetime (ns)
organic dye (Alexa 488)	3.10^{-16}	~75000	0.92	7×10^5	~40	few seconds	~4 ns
quantum dot	$\sim 1.10^{-14}$ (ref 81,82)	$\sim 2 \times 10^6$	0.3—0.5 (ref 81,83)	1×10^7	~30 (ref 81)	>1000 s	~10 ns (ref 84)
rare-earth nanoparticle (30 nm $Y_{0.6}$ $Eu_{0.4}VO_4$ particles with ~60000 emitters)	2.10^{-16}	~50000	0.16	1×10^5	~10 (ref 32)	>1000s	~300 μs (ref 57,80)
nanodiamonds (with 3NV centers)	9.10^{-17} (ref 85)	~25000	*0.99* (ref 86)	$<3 \times 10^5$	~75 (ref 85)	>1000 s	~10 ns (ref 85)

[a] The absorption cross-section for A488, Quantum dots (bare 3 nm CdSe[82] or core-shell CdSe/Zns,[81] 3 nm core radius), YVO_4:Eu nanoparticles and nanodiamonds were measured with respective excitations of 488, 500, 466, and 523 nm. Emission rate and time before photobleaching are estimated for a nonsaturating excitation intensity of 1 kW/cm^2 and with a typical number of photons emitted before photobleaching of 10^6 for A488. Note that A488 is one of the brightest organic fluorophores. All data concerning A488 are available in the documentation provided by the Invitrogen company. Note that the photon emission rate for quantum dots does not take into account the absence of emission when the dots are in a dark state (blinking). For nanodiamonds, the quantum yield was measured in bulk material and is probably weaker in nanoparticles. Furthermore, note that a broad emission spectrum is unfavorable for efficient detection in the presence of a fluorescent background. Thus, the photon emission rates presented in the table likely notably overestimate the number of photons that can be collected. Finally, these values concern bare particles and fluorophores and may be lower after functionalization and coupling to biomolecules.

nanoparticles such as $NaYF_4$:Yb,Er or $NaGdF_4$:Yb,Er.[38,39,63] Recently, a highly crystalline YVO_4 matrix has also proven promising.[69] Two-color lymphatic imaging was furthermore performed using two rare-earth dopant pairs Yb/Er and Yb/Tm in $NaYF_4$ nanocrystals.[39]

The forbidden nature of the transitions among different f-electron configurations leads to very long excited state lifetimes (~1 ms) compared to the lifetime of organic fluorescent probes (~1 ns). As a consequence, the brightness (the number of emitted photons per unit time) of a single emitting center is much lower than that of organic fluorophores or quantum dots. However, in a single nanoparticle several hundreds or thousands of ions contribute to light emission, so that a single nanoparticle is detectable under biologically compatible laser illumination with a CCD camera.[32,70,71] In addition, the long lifetimes can be exploited for easy implementation of retarded detection schemes eliminating undesired signals like cell background fluorescence and direct acceptor excitation in Förster resonant energy transfer (FRET) experiments.[32,71] $Ca_{0.2}Zn_{0.9}Mg_{0.9}Si_2O_6$:($Eu^{2+}$, Dy^{3+}, Mn^{2+}) nanoparticles present extremely long fluorescence decay times (~100 s). The order of magnitude of the persistence of the luminescence enables experiments with extemporaneous excitation of nanoparticles and imaging without excitation. This can be fruitful for *in vivo* imaging[42] to minimize background.

Strictly speaking, the brightness limitation is not due to the lifetime but to the extinction coefficient and the quantum yield. When one of the electric-dipole forbidden rare-earth ion transitions is used for the excitation, the extinction coefficients are relatively low compared to quantum dots (10^5—10^6 $cm^{-1}\cdot M^{-1}$) but are comparable to those of organic fluorophores (Table 1). For direct excitation of Eu^{3+} ions at the $^7F_{0,1}$—$^5D_2$ transition at 466 nm, for example, the extinction coefficient is 50000 $cm^{-1}\cdot M^{-1}$ for 30-nm $Y_{0.6}Eu_{0.4}VO_4$ nanoparticles.[32] For excitation of the matrix, on the other hand, the extinction coefficient is much higher.[32] Efforts during synthesis may increase the nanoparticle brightness, for example by annealing[72,73] or microwave treatment.[74]

One of the main disadvantages of organic dyes is their fast (a few seconds under ~1 kW/cm^2 of resonant illumination) and irreversible transition to a dark state, or photobleaching. Quantum dots, on the other hand, show blinking at the single particle level that can only be avoided with highly specific growth procedures.[78,79] This blinking feature is completely absent from rare-earth based nanoparticles due to the presence of a large number of emitters in each particle.[32,40,63,69] The luminescence of rare-earth nanoparticles under illumination is higly stable: In most cases the luminescence remains unchanged (Figure 1C)[76] while a partial decay is observed, for Eu^{3+}-doped nanoparticles, for example (Figure 1D).[32,77] This decay has been proven to be reversible and due to the photoinduced reduction of Eu^{3+} to Eu^{2+} (Figure 1D).[77] In both systems, the photostability allows the continuous observation of rare-earth nanoparticles for arbitrarily long durations.[63,76,80,69] Furthermore, the oxido-reduction processes observed in YVO_4:Eu nanoparticles have been exploited to demonstrate an oxidant sensor for hour-long experiments (see subsection Oxidant Nanoprobes and ref 77). This variability in optical properties (rate of photon emission, photostability, *etc.*) due to the chemical nature of the nanoparticles makes them suitable for different applications at the single particle level and as volume labels, for example, for *in vivo* applications. These different applications are detailed below.

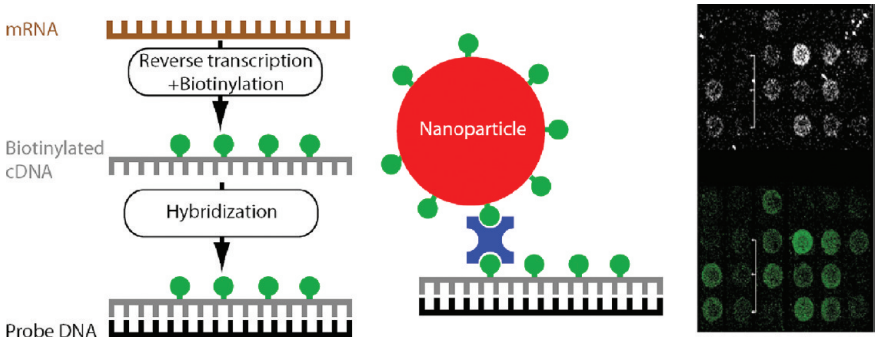

Figure 2. DNA detection with upconversion nanoparticles. (Left) Scheme for the DNA labeling with nanoparticles on microarrays. These experiments were made with nanoparticles coated with silica and functionalized with amino groups and biotin. Biotin is indicated in green and neutravidin in blue. cDNA with biotinylated nucleotides is first synthesized by reverse transcription (top left). Hybridization with complementary probe DNA grafted on the microarray (bottom left) is then revealed by the binding of neutravidin-coated fluorescent nanoparticles (center). (Right) Microarray labeled with Cy5 (top) and Y_2O_2S:Yb,Er nanoparticles (bottom). Note the three spots indicated by white lines, that are only detected through nanoparticle imaging. Results reprinted with permission from ref 36. Copyright 2001 Nature.

Magnetic Properties. Several rare-earth ions have a large number of unpaired electrons and thus provide high magnetic moments under a magnetic field. Gd^{3+} and Eu^{2+} ions with seven unpaired electrons yield the highest magnetic moments and can thus be used to decrease the longitudinal relaxation time T_1 of water protons in a strong static magnetic field after a resonant radiofrequency excitation. Gd^{3+}, due to its higher availability and chemical stability, is thus widely used as a contrast agent for magnetic resonance imaging (MRI). Applications of Gd-based nanoparticles to MRI and their comparison with commercial Gd-complexes are detailed below in the subsection titled Contrast Agents for MRI Imaging.

Cytotoxicity. The cytotoxicity of Cd-containing quantum-dots is mostly due to a potential release of free cadmium and depends on their surface functionalization.[87,88] This is an important limitation of their use for biomedical applications and justifies research for others semiconductor compounds (InP, $CuInS_2$). For different types of rare-earth nanoparticles, with or without functionalization, no cytotoxicity was observed.[62,77,89] For example, gadolinium oxide particles injected in mice were naturally eliminated by renal excretion after a few hours without any damage to the animal,[62] and YVO_4:Eu nanoparticles internalized in vascular cells induce no mortality hours after their internalization.[77] The potential toxicity of each type of nanoparticle depends on its constituent materials and on the chemical properties of its surface coating and the size of the particles.[90] Therefore, further experiments as a function of coating and constituent materials are necessary before any general assessments can be made.

BIOCHEMICAL APPLICATIONS

DNA Assays. Rare-earth nanoparticles have been used for DNA detection following two different approaches: the use of DNA-sensitive nanoparticles and the use of nanoparticles as labels of DNA fragments.

LaF_3:Ce^{3+},Tb^{3+} nanoparticles of ~50 nm radius coated with polymers are fluorescent mostly due to to Tb^{3+} transitions. This fluorescence can be quenched by the presence of nucleic acids such as DNA. This is possibly due to the formation of hydrogen bonds between DNA and carboxylic acids of the nanoparticle polymer coating enabling energy transfer from excited Tb^{3+} to DNA. It is thus possible to determine DNA concentration by measuring the fluorescence intensity. Concentrations as low as 2 μg/mL have been detected:[34] this compares favorably to conventional measurements performed with a spectrophotometer.

DNA microarrays or DNA chips are widely used to study mRNA expression patterns. This technology relies on the hybridization of probe DNA strands spotted on a chip with a fluorescently labeled target DNA, usually obtained by reverse transcription of mRNA extracted from cells. The fluorescence intensity reveals the quantity of the complementary fragment of each probe. The commonly used fluorophores are cyanine dyes (Cy3 and Cy5). This method has been advantageously replaced by biotinylation of target DNA followed by labeling with neutravidin-coated Gd_2O_3:Eu[91] or with upconversion nanoparticles Y_2O_2S:Yb,Er[36] (Figure 2). Concentrations of target DNA as low as 1 ng/mL were detected, which is a 5 times improvement compared to Cy5 labeling. Weakly expressed mRNA, undetectable by usual methods, has thus been revealed in a sample extracted from a bladder carcinoma[36] (Figure 2).

Detection of single nucleotide polymorphisms (SNPs) is important for the diagnosis of different diseases, such as polycystic kidney disease (PKD), and is usually based on quantitative RT-PCR (reverse transcription polymerase chain reaction), which is a time-consuming and expensive method. Fe_3O_4/Gd_2O_3:Eu nanoparticles[33,91] consisting of a Fe_3O_4 core and a Gd_2O_3:Eu shell are fluorescent due to the presence of Eu^{3+} ions and magnetic due to the magnetite core, and

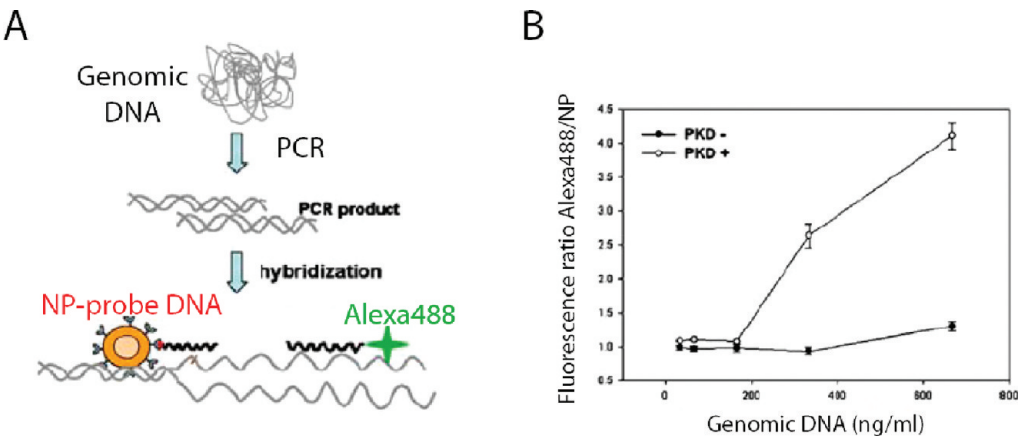

Figure 3. Detection of single nucleotide polymorphisms. (A) Method for purification of target DNA. DNA fragments with (+PKD) or without a mutation (−PKD) of interest are amplified by PCR then hybridized with Alexa488-labeled DNA and probe DNA (complementary of the +PKD mutated strand) coupled to Fe_3O_4/Gd_2O_3:Eu nanoparticles. After that treatment, only +PKD fragments are labeled both by the nanoparticle and the fluorophore. Purification is then achieved by a magnet due to the magnetic properties of the nanoparticles. The ratiometric detection of A488 fluorescence (compared to nanoparticle fluorescence) in the purified sample then reveals accurately the presence of the target DNA. (B) Fluorescence ratio for +PKD and −PKD samples: significant detection for [DNA] > 200 ng/mL. Reprinted with permission from ref 92. Copyright 2008 Springer Science+Business Media.

they have been successfully used to detect SNPs.[92] Nanoparticles were functionalized with neutravidin and then coupled to probe DNA fragments (complementary of the target DNA carrying the +PKD mutation). Genomic DNA was then extracted from tissue and the region of interest containing the polymorphism was amplified by PCR and hybridized—for both −PKD and +PKD samples—with a complementary strand labeled by an organic dye (Figure 3A). When probe DNA coupled to nanoparticles and sample DNA are mixed, hybridization occurs preferentially for the correct SNP. Hybridized fragments containing nanoparticles are separated from the solution by a magnet and the luminescence ratio between Eu^{3+} and organic dye reveals the fraction of bound DNA. The presence of a given polymorphism is thus detected by the measurement of the fluorescence ratio (Figure 3B). The combination of magnetism for separation and of fluorescence for quantification using the reference signal of the organic dye yields a powerful method for quantitative detection of SNPs.

Protein Detection. *In vitro* detection of proteins by fluorescent or radioactive labels in immunoassays is important either for molecular biology experiments or for diagnosis. Lanthanide chelates or cryptates are already commonly used and commercially distributed in that context (dissociation-enhanced lanthanide fluorescence immunoassay) as an improvement to conventional ELISA (enzyme-linked immunoabsorbent assay). These applications rely on the ensemble detection of fluorescence of europium chelates under UV excitation to improve sensitivity.[93,94] The development of nanoparticle-based methods is however essential to achieve single molecule detection either for ultrasensitive *in vitro* detection or for applications where *in vivo* single protein imaging is required (see below).

Europium-doped gadolinium oxide nanoparticles were used to detect protein micropatterns.[75] Biotin was regularly patterned on a silicon wafer by microcontact printing and nanoparticles were coated with streptavidin, able to specifically bind biotin. After 1 h incubation and rinsing of the unbound particles, the pattern was observed by fluorescence microscopy (Figure 4A). This experiment demonstrated the feasibility of efficient protein detection on a substrate and could be used as a model for biologically relevant problems using antibody-coated nanoparticles. The possibility to use rare-earth nanoparticles in immunoassays instead of organic dyes was demonstrated by labeling mouse IgG with $NaYF_4$:Yb,Er nanoparticles coupled to antimouse antibodies (Figure 4B).[38]

Nanoparticles with organic cores have also been successfully used for sandwich-type immunoassays.[54] As in standard ELISA protocols, prostate specific antigen (PSA) or thyroid stimulating hormone (TSH) were incubated and bound in microwells coated with specific antibodies. Europium-chelate-doped polystyrene nanoparticles were coated with specific antibodies against PSA or TSH in order to probe the bound antigen in microwells. Nanoparticle fluorescence was then detected at 615 nm through a fluorimeter to reveal the presence of the antigen. The comparison between nanoparticle labeling and soluble dye revealed that specificity is mostly determined by antibodies,[54] while sensitivity can notably be increased by the use of nanoparticles.[53]

These applications—DNA detection or protein immunodetection—are routine procedures in biology laboratories. The advantage of rare-earth nanoparticles is to provide a qualitative improvement of existing assays based on the rare-earth photostability, efficient detection, and facile coupling of magnetic and luminescent properties.

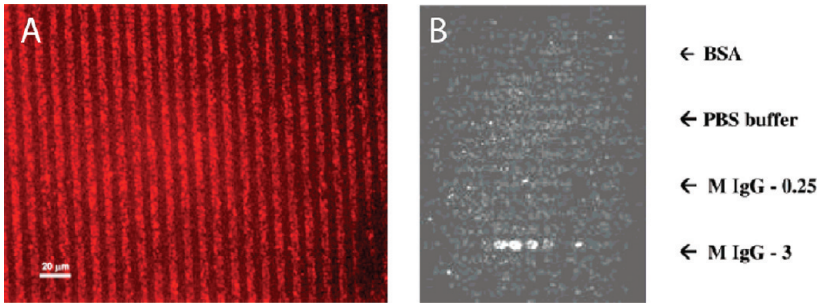

Figure 4. Protein detection on micropatterns. (A) Pattern of biotin revealed by the nanoparticle luminescence. Reprinted with permission from ref 75. (B) Immunoassay: the presence of mouse IgG was revealed by the emission of nanoparticles coupled to antimouse antibodies (line 4). No nonspecific binding to controls lines (line 1 and 2) was observed. Reprinted from ref 38. Copyright 2002 American Chemical Society.

FRET. Fluorescence resonant energy transfer (FRET) has become a widely used technology in biology using different types of materials for the detection of protein–protein interactions.[95] This method relies on the efficient energy transfer of an excited fluorophore labeling one protein (the donor) to the fluorophore labeling a second protein (the acceptor) and on the ability to specifically detect the fluorescence resulting from this process. It is thus important to efficiently discriminate this signal from direct acceptor excitation and donor emission leaking in the acceptor channel. Lanthanide nanoparticles are promising donors for FRET applications (more rigorously termed LRET in the case of lanthanide ions for luminescence resonant energy transfer) for multiple reasons.[21] First, the large Stokes shift of lanthanide systems allows excitation at much shorter wavelength than the acceptor absorption and thus prevents its direct excitation. Second, the narrow emission lines of lanthanide nanoparticles limit the overlap with the acceptor emission spectrum. Third, the absence of photobleaching facilitates the FRET experiments. Fourth, the long (~1 ms) lifetime of the excited states in lanthanide systems allows easy detection of donor lifetime changes due to FRET (Figure 5A). Indeed, a simple setup with a mechanical chopper and a numerical oscilloscope is sufficient for these lifetime measurements. In addition, these long lifetimes lead the acceptor emission due to FRET to occur at longer time scales than direct fluorescence of an organic fluorophore acceptor (~1 ns) and enables an easy separation in time-resolved FRET experiments.[71]

Such properties were already obtained by using soluble europium chelates and cryptates as a donor allowing a UV excitation in ensemble experiments.[21,94,96–98] In addition, their long lifetimes have been exploited to demonstrate FRET applications with quantum dots (QDs) as acceptors despite the QD broad absorption spectrum thus yielding a robust photostable FRET system.[22] Micrometric melamine nanoparticles have been coated by several layers of europium chelate to detect proteins.[99] The proposed method is based on the competition between adsorption of fluorescently labeled BSA and target protein on the nanoparticles. In the absence of protein, labeled BSA at the surface of the particle is excited by FRET. The decrease of the FRET signal in the presence of proteins replacing labeled BSA is thus a function of protein concentration. Typical concentrations of 100 $\mu g \cdot L^{-1}$ of BSA, γ-globulin or thyroglobulin were thus detected. These performances are comparable with commercial protein titration methods. Similarly, europium-chelate-doped polystyrene beads were used for FRET experiments to detect cells and probe their viability in solution.[100] In that case, labeled BSA adsorption is prevented by the presence of cells, resulting in a FRET signal decrease depending on the number of cells in solution. The sensitivity of this method was sufficient to count five cells in solution in a microwell, which is significantly less than that of standard automated counters.

Experiments performed with Cy5 acceptors adsorbed onto YVO_4:Eu donor nanoparticles also illustrated the efficiency of the use of nanoparticles: FRET was revealed by a significant alteration of both the nanoparticle and the Cy5 fluorescence decay (Figure 5 panels A and B, respectively).[71] These experiments show the efficiency of rare-earth nanoparticles as FRET donors for biological applications by detecting the proximity of a fluorophore commonly used in living systems. Furthermore, the possibility of observing FRET using a single rare-earth nanoparticle donor was demonstrated.[71]

Upconversion nanoparticles, usually made by codoping with Er^{3+} and Yb^{3+}, also have an interesting potential as donors in FRET applications.[101,102] Their anti-Stokes shift indeed allows FRET with an excitation wavelength longer than that of acceptor emission and thus a clean detection of a specific FRET signal. These particles have been used in different biological contexts. Nanoparticles were coated with streptavidin and mixed with a biotinylated protein labeled with a fluorescent acceptor,[101] whose fluorescence was detected after infrared excitation of the donor nanoparticles: this demonstrated the feasibility of protein detection with FRET from upconversion nanoparticles. This has been applied *in vitro*[103] and for diagnosis[104] for the detection of estradiol (E2) by a competitive

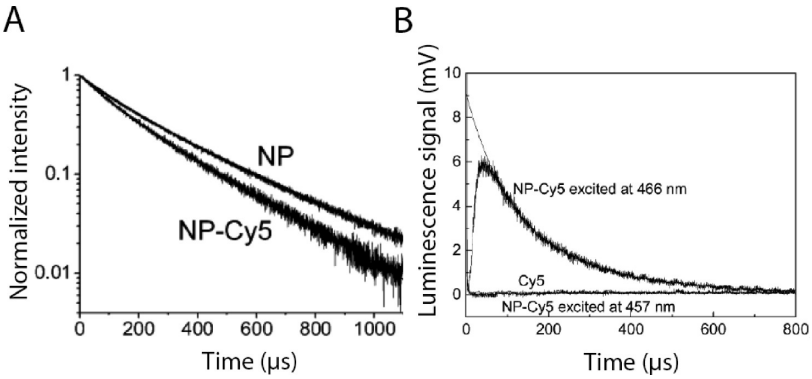

Figure 5. Fluorescence resonant energy transfer using YVO_4:Eu nanoparticles as donors and Cy5 fluorophores as acceptors. Direct excitation of Eu^{3+} ions at 466 nm. (A) Fluorescence decay (617 nm) for bare nanoparticles (NP) or nanoparticles coated with Cy5 (NP-Cy5). Note the faster decay of fluorescence for NP-Cy5, revealing FRET. (B) Fluorescence decay in the Cy5 emission channel (670 nm) of free or NP-bound Cy5. A pair of synchronized mechanical choppers enables starting the detection 50 μs after the excitation beam has been blocked. Thus, no signal is observed for a free Cy5 solution under Eu^{3+} excitation indicating efficient rejection of direct Cy5 (acceptor) excitation with the donor excitation wavelength. The excitation of NP-Cy5 shows a long emission lifetime determined by the donor lifetime as expected for FRET emission.[21] The absence of signal for nonresonant nanoparticle excitation (457 nm) confirms the exclusive detection of the FRET signal without any contributions from direct acceptor excitation. The two zero-signal curves (Cy5 and NP-Cy5 under 457 nm excitation) are indistinguishable. The thin black line is a biexponential fit of the NP-Cy5 signal. Reprinted from ref 71. Copyright 2006 American Chemical Society.

immunoassay. $La_2O_2S:Er^{3+},Yb^{3+}$ nanoparticles were coated with E2 antibody and mixed with E2 coupled to an acceptor fluorophore (E2-AF680), which creates FRET signal. After addition to a blood sample, there is a competition between native E2 from the blood and labeled E2, causing a reduction of FRET (Figure 6A,B). Concentrations in the nanomolar range have thus been detected.[104] This application is particularly interesting for blood testing, because of its sensitivity and the small sample volume required for the experiment. A similar approach was used to quantify an endonuclease activity. Nanoparticles were coated with a nucleotide coupled to a fluorescent acceptor (AF680) and a quencher (nonfluorescent acceptor) at its ends.[105] Thus, this conjugate does not emit in the acceptor channel (Figure 6C). When the nucleotide is cleaved by the endonuclease, the quencher is released and FRET signal is restored depending on the endonuclease concentration. (Figure 6D).[105] As a consequence, this allows a quantitative monitoring of the protein activity. Interestingly, this assay is not a competitive assay and provides a direct activity measurement, without any requirement of labeling the protein of interest. Although direct excitation of AF680 as a donor could allow the same kind of measurements, the use of upconversion nanoparticles notably reduces the background due to their anti-Stokes shift.

CELL BIOLOGY AND IN VIVO APPLICATIONS

Nonspecific Imaging. The simplest applications of rare-earth nanoparticles in living systems are nonspecific loadings of nanoparticles in living cells or organisms. These experiments illustrate their remarkable optical properties and their absence of cytotoxicity and provide instrumental developments likely to contribute to specific protein imaging *in vivo*. Upconversion nanoparticles are particularly interesting in that perspective, due to the absence of fluorescence background coming from the external medium.[39,76,107] Moreover, infrared excitation is interesting for imaging of tissues due to their low absorption in biological media. Y_2O_3:Yb,Er nanoparticles have thus been used for imaging of the *Caenorhabditis elegans* worm.[107] Particles were added to worm food, ingested without damage for the worm, and imaged by infrared excitation. This provides images of the worm digestive system (Figure 7A).[107]

Experiments combining uptake of nanoparticles and confocal microscopy have been proposed[76,108] in cell cultures and *in vivo*. $NaYF_4$:Yb,Er particles have been loaded in HeLa cells[108] or mouse skeletal myoblasts[76] in culture by incubation. This allows the tracking of single cells *in vitro* and *in vivo* after injection of these loaded cells in a mouse vein or intramuscular injection of nanoparticles (Figure 7B).[76] The anti-Stokes shift of upconversion nanoparticles provides a sufficient contrast for imaging at a depth of ~2 mm, which is comparable to performances obtained in 2-photon microscopy.

Intravenous injection of persistent luminescence $MgSiO_3:Eu^{2+},Dy^{3+},Mn^{2+}$ particles in living mice has enabled *in vivo* imaging of different organs during 1 h without need for excitation after injection.[42] Interestingly, the coating of these nanoparticles determines which organs are labeled: this is the first step toward targeting for specific imaging (Figure 7C).

Specific Protein Targeting. The labeling of proteins with fluorescent tags in cells or tissues has become a major tool of cell biology. It is widely used in fixed cells in immunocytochemistry for the study of cell organization. The existing diversity of organic dyes is rather

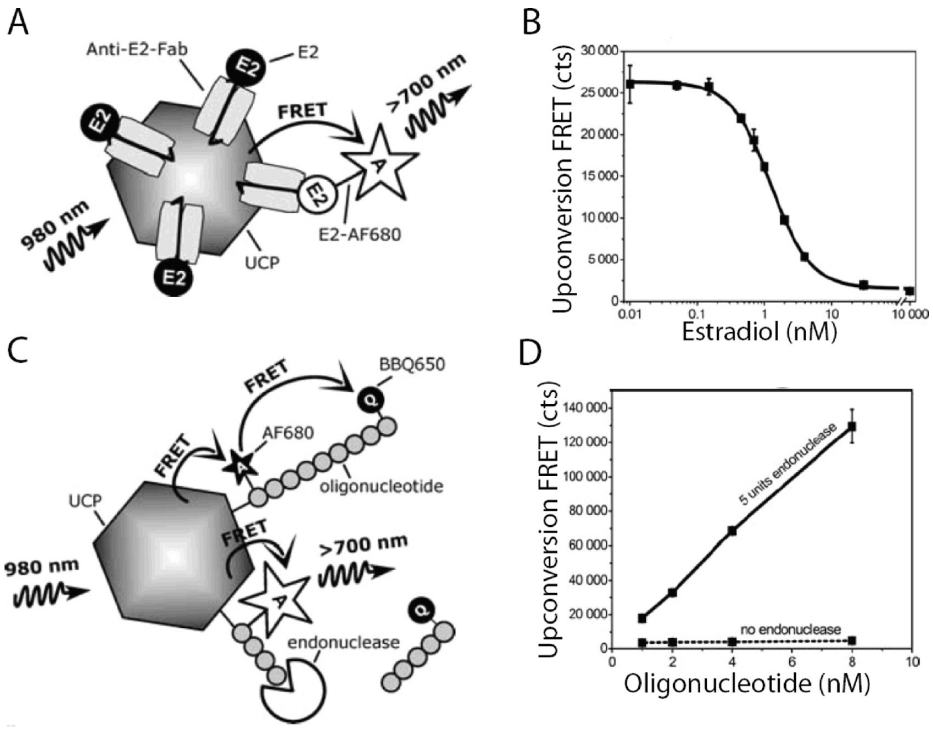

Figure 6. FRET-based estradiol and endonuclease activity detection using upconversion nanoparticles as donors. (A) Upconversion nanoparticle (UCP) functionalized with Anti-E2 antibody. There is a competitive binding of native E2 (black) and acceptor-coupled E2 (white) responsible for FRET. (B) FRET signal as a function of native E2 concentration. (C) Upconversion nanoparticle coupled to an oligonucleotide containing at its two ends an acceptor (A) and a quencher (Q). Successive energy transfer from the upconversion nanoparticle to the acceptor and from the acceptor to the quencher leads to fluorescence quenching for uncleaved oligonucleotides. The fluorescence is restored when the quencher is released by cleaving of the oligonucleotide. (D) FRET signal as a function of the oligonucleotide concentration with and without endonuclease. Reprinted with permission from ref 106. Copyright 2008 John Wiley & Sons, Inc.

sufficient for that purpose. However, the visualization of proteins in a living cell is slightly more difficult because of the fast photobleaching of GFP variants or of organic dyes. In this domain, rare-earth-doped nanoparticles can contribute notably to biology, because of their remarkable photostability and absence of emission intermittency. Nanoparticles can be functionalized (with an antibody or a ligand) to specifically bind a protein. YVO_4:Eu nanoparticles functionalized with epoxy groups were coupled to guanidinium groups (Figure 8A).[32] These groups are responsible for the inhibition of voltage-gated sodium channels by saxitoxin and tetrodotoxin (neurotoxins secreted by marine microorganisms).[109] When these nanoparticles are added to the culture medium of frog cardiomyocytes, they bind to the pore opening of sodium channels and thus allow their imaging through laser excitation of Eu^{3+} ions at 466 nm (Figure 8B). The long lifetime of nanoparticle fluorescence enabled a time-gated detection: two synchronized choppers (one for the source, the other for the camera) induce a $\sim 50\,\mu s$ delay between the end of the illumination and the beginning of the acquisition. This eliminates the cell fluorescence and is a major advantage of long-lifetime fluorescent probes. It has thus been possible to image sodium channels with single molecule resolution in living cells (Figure 8B).

The targeting of a specific protein in a living cell with a nanoparticle (quantum dots or rare-earth doped nanoparticles) has been, however, so far mostly restricted to membrane proteins. Unbound nanoparticles can indeed be rinsed while specifically bound nanoparticles stay at the cell membrane by recognizing their target protein. Rinsing is not possible inside the cell which prevents this approach for cytosolic proteins. An interesting approach for that purpose is the external nanoparticle labeling of purified proteins followed by the purification of nanoparticles bound to a functional protein and their subsequent injection into the cell. The reliability of this method depends on the extreme purity of the injected sample: any unbound nanoparticle would cause an artifact. It has been used only for quantum dots up to now for a very particular system—single kinesin imaging—for which specific purification methods exist.[110] Strictly speaking, this method does not target cytosolic proteins but injects labeled proteins in the cytosol. The possibility to label intracellular proteins with nanoparticles thus remains a major challenge. Organic fluorophores have been used to target genetically modified cytosolic proteins.[111] While such approaches can also be envisaged for nanoparticles, particular caution in terms of size is required to avoid artifacts due to the molecularly crowded intracellular environment.[112]

Single-Protein Tracking. For several years, there has been a growing interest in single molecule imaging in living cells, particularly for membrane proteins.[5,113−115] Their tracking indeed reveals important information on the cell membrane properties and organization or the interactions with other proteins. The use of quantum dots has become quite popular, although their blinking causes the trajectory reconstruction to be complex.[116,117] Nonblinking YVO_4:Eu particles have been used to track

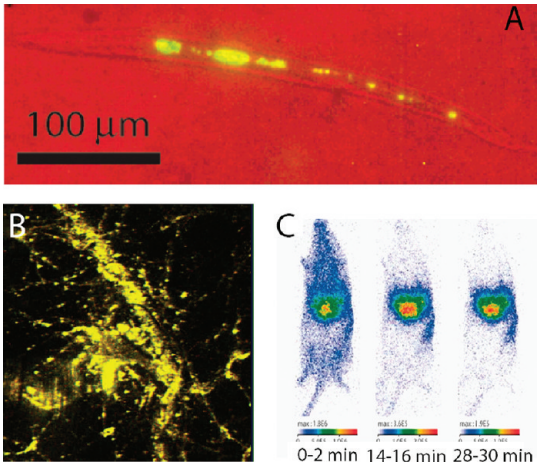

Figure 7. (A) Nonspecific imaging with upconversion nanoparticles. *C. Elegans* worm after Y_2O_3:Yb,Er nanoparticle ingestion for 24 h (nanoparticles appear in green) revealing the worm digestive system. Reprinted from ref 107. Copyright 2006 American Chemical Society. (B) Projection of a 2 mm thick stack of a mouse hind limb after injection of myoblasts with internalized $NaYF_4$:Er,Yb nanoparticles. Reprinted with permission from ref 76. Copyright 2009 Elsevier. (C) Images of carboxyl coated $Ca_{0.2}Zn_{0.9}Mg_{0.9}Si_2O_6$:-($Eu^{2+}$, Dy^{3+}, Mn^{2+}) nanoparticles injected to a living mouse. Owing to persistent luminescence, images were obtained without excitation. Reprinted with permission from ref 42. Copyright 2007 National Academy of Science, USA. The nanoparticles accumulated preferentially in the liver.

ε-toxin receptors in the membrane of Madin−Darby canine kidney (MDCK) cells (Figure 9).[80,118] Functionalization by amine groups followed by coupling to the toxin[56,57] leads to the binding of the nanoparticles to the membrane receptors. Single-particle detection has also been demonstrated with upconversion particles;[40,63,69] the specific binding to single biomolecules, however, still remains to be shown.

The coupling ratio between nanoparticles and proteins is essential to achieve single molecule measurements. Therefore, Casanova *et al*. proposed a method based on the single-step photobleaching of proteins labeled with organic fluorophores to determine the exact number of proteins bound to single nanoparticles.[56] This was demonstrated for YVO_4:Eu nanoparticles but the approach is applicable to any type of particle. In practice, when the mean ratio is close to 1:1, it is unlikely for a single particle to bind more than one receptor.[110,118] In that case, a single nanoparticle trajectory reliably reflects the trajectory of a single receptor. The viscosity difference between the outer medium and the cell membrane ensures that the observed motions are not hindered by the size of the nanoparticles. This was confirmed in different systems by comparing diffusion coefficients of nanoparticle-labeled and organic dye-labeled proteins.[80,117] Owing to the photostability and absence of blinking of the nanoparticles, several minute-long uninterrupted trajectories with a 20−50 ms resolution and a localization precision down to 20 nm were recorded (Figure 9). It should be noted that a minimum nanoparticle size is required for these applications so that the numbers of photons emitted during the short acquisition times, which are proportional to the nanoparticle volume,[70] are detectable above the background. Typically, YVO_4:Eu nanoparticles with sizes of 30 nm or above were required, sizes comparable to those of commercial quantum dots.

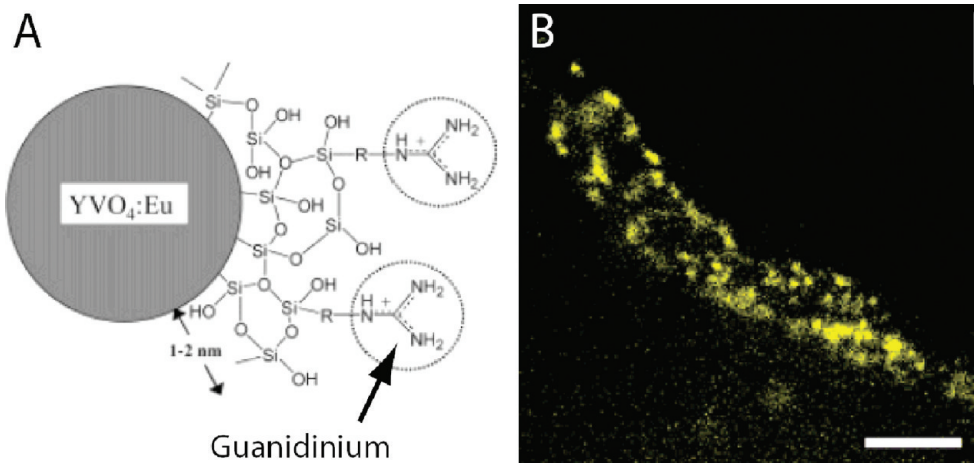

Figure 8. Labeling of voltage-gated sodium channels using YVO_4:Eu nanoparticles. (A) Nanoparticle functionalized with guanidinium groups able to bind sodium channels. (B) Fluorescence image of a living frog cardiomyocyte. Yellow dots are nanoparticles labeling voltage-gated sodium channels. Diffusion limited spots are single nanoparticles. Scale bar: 5 μm. Reprinted from ref 32. Copyright 2004 American Chemical Society.

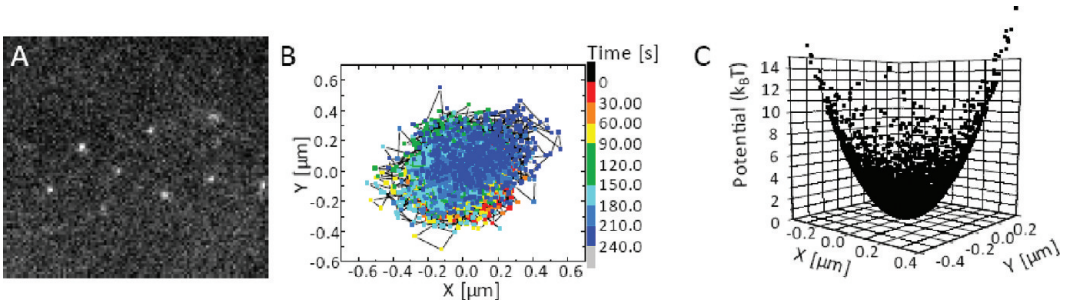

Figure 9. Single toxin receptor tracking using YVO_4:Eu nanoparticles.[80,118] (A) Fluorescence image of single toxin receptors in the membrane of MDCK cells labeled by YVO_4:Eu nanoparticles. (B) Example of a reconstructed trajectory. Confinement can be observed. (C) Potential felt by the receptor describing the trajectory shown in panel B.

Using single-molecule tracking data obtained with rare-earth-doped nanoparticles, it was not only possible to measure the diffusion coefficient, which is also accessible by tracking of organic-dye labeled proteins, but also to reconstruct the force field of the microdomain in which the toxin receptor was moving using a novel approach based on Bayesian inferences[80,118] (Figure 9). This is an illustration of the exciting possibilities provided by the use of nanoparticles in biology: their remarkable optical properties not only facilitate previously possible experiments but also give access to entirely new biologically relevant information.

Oxidant Nanoprobes. The detection of intracellular signaling molecules is an essential requirement in cell biology. H_2O_2 is implicated in signaling in a variety of physiological cellular processes (contraction, migration, proliferation, differentiation, apoptosis, *etc.*) and plays an important role in pathophysiological conditions like atherosclerosis, inflammatory processes, and neurodegenerative and malignant diseases. The ability of the cell to produce distinct responses to signals sharing the same secondary messenger is currently poorly understood due to the lack of accurate and dynamic methods to measure the intracellular response.

Recent experiments using rare-earth nanoparticle imaging have contributed to this field by the quantitative and dynamic measurement of H_2O_2 concentration in living cells.[77] The main emission of YVO_4:Eu nanoparticles is due to the $^5D_0-^7F_2$ transition of dopant Eu^{3+} ions centered at 617 nm. Eu^{3+} ions can be reduced to Eu^{2+} ions through a photoinduced mechanism (Figure 10A). A relatively high intensity resonant illumination for 250 s is thus sufficient to induce an important fluorescence decrease (~70%, Figure 10A). The subsequent *in vitro* application of H_2O_2 causes an oxidation of Eu^{2+} and consequently a recovery of the fluorescence at 617 nm (Figure 10A,B). This recovery amplitude and speed depends on the applied H_2O_2 concentration (Figure 10B,C). Furthermore, this recovery is reversible (Figure 10A) and no aging of the nanoparticles was revealed: their response is identical whatever the history of the oxidation state was.[77] Altogether, these results allow the determination of a law relating the instantaneous concentration of H_2O_2 to the fluorescence signal:

$$S(t)/S(0) = A[C(t)](1 - \exp(-\frac{t}{\tau[C(t)]}))$$

This enables the *in vitro* dynamic and quantitative measurement of H_2O_2 concentration (Figure 10D). The response of YVO_4:Eu nanoparticles is not specific to H_2O_2, and similar fluorescence recovery can be obtained with other oxidant species. These particles can thus probably also be used for the detection of other physiological oxidants such as ClO^- or NO.[77]

Nanoparticles were internalized in vascular smooth muscle cells (VSMCs) by pinocytic loading to dynamically measure the intracellular H_2O_2 concentration (Figure 11). No cytoxicity due to the nanoparticles within the cell was observed: after 18 h, the proportion of living cells was equal to that obtained in the absence of nanoparticles.[77] This highlights one of the major advantages of rare-earth doped nanoparticles compared to other methods of intracellular labeling enabling harmless long-term imaging and likely *in vivo* applications.

In response to stimulation by endothelin-1 (ET-1) or platelet derived growth factor (PDGF), VSMCs produce H_2O_2 through the activation of the NADPH oxidase (NOx)protein complex leading, respectively, to contraction or migration. The produced quantities of H_2O_2 were similar (7 μM). The timing of the production, however, was notably different. These differences are important in relationship with the signal transduction in living cells and more specifically for understanding the ability of the cell to discriminate between different signals sharing common second messengers. These measurements were enabled by the unique oxido-reduction properties of rare-earth-based nanoparticles.

The H_2O_2 production in the vascular system was quantified over time: this result is only accessible by rare-earth nanoparticle imaging. Alternative methods using either organic oxidant indicators such as DCF (DiChloroFluorescein),[2] Amplex Red (Invitrogen), or a genetically encoded sensor (Hyper protein)[119] only provide qualitative information due to their lack of

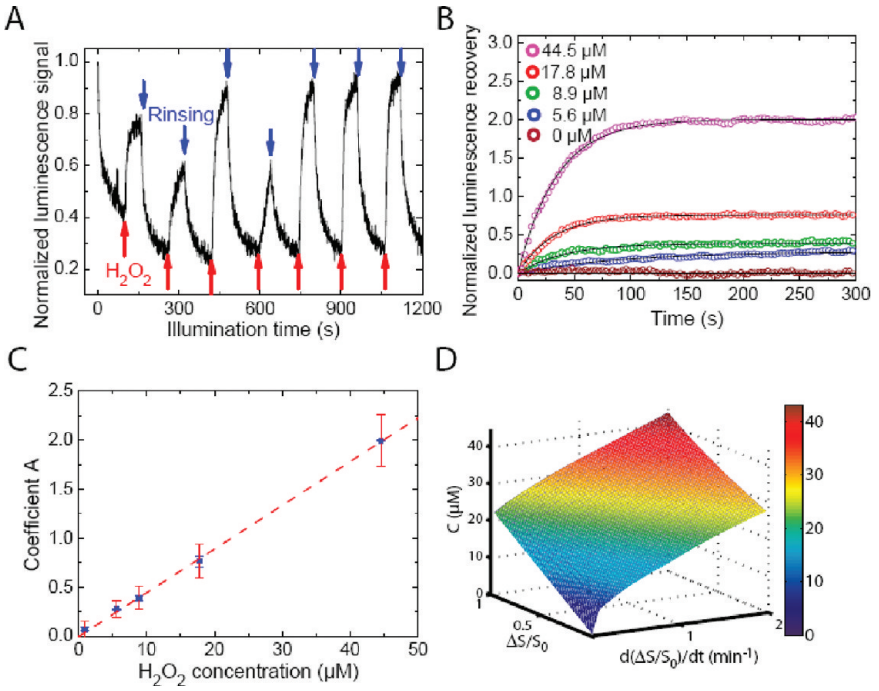

Figure 10. *In vitro* H_2O_2 detection using YVO_4:Eu nanoparticles. (A) Cycles of photoreduction and chemooxidation. The cycles number 2 and 4 are obtained for a H_2O_2 concentration half that for other cycles. (B) Fluorescence evolution after photoreduction and subsequent addition of H_2O_2 at $t = 0$ at different concentrations (average of ~20 single nanoparticles). (C) Amplitude of fluorescence recovery as a function of H_2O_2 concentration determined from exponential fits of the curves in panel B. Blue bars indicate the error bar of the fit and red bars the standard deviation of fits performed on single nanoparticle measurements. (D) Instantaneous H_2O_2 concentration as a function of fluorescence signal and its first temporal differential. Reprinted from ref 77. Copyright 2009 Nature.

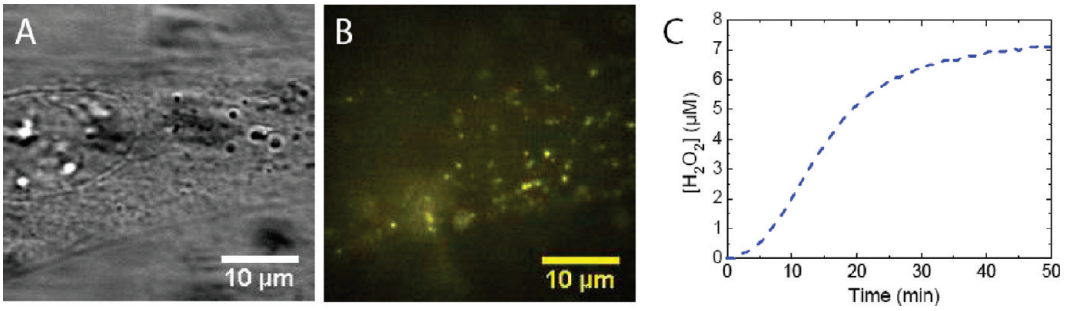

Figure 11. H_2O_2 detection in living cells using YVO_4:Eu nanoparticles. (A) White-light transmission image of a vascular smooth muscle cell loaded with nanoparticles. (B) Fluorescence image of internalized nanoparticles in the same cell. (C) Response to a 100 ng/mL PDGF stimulation. Reprinted from ref 77. Copyright 2009 Nature.

reversibility or quantitativity. In addition, the spatial accuracy in $[H_2O_2]$ measurements is only limited by the positioning error of the nanoparticles. Using standard methods for single particle tracking, it is thus possible to detect H_2O_2 in living cells with an accuracy of 50 nm, 0.2 μM, and 30 s.

Contrast Agents for MRI Imaging. Magnetic resonance imaging (MRI) is one of the main modalities for medical imaging, notably because it is not invasive and enables in-depth 3-dimensional imaging. The pulse MRI technique relies on the relaxation of water protons in a strong static magnetic field after a pulse of transverse radiofrequency field. The longitudinal and transverse relaxation times T_1 and T_2 of the magnetization used for image reconstruction are highly affected by the environment. Superparamagnetic iron oxide nanoparticles[120] shorten these relaxation times, mostly the T_2-time, and are commonly used to locally darken T_2-weighted MRI images (positive contrast agents). On the other hand, the presence of paramagnetic species with unpaired electrons is known to notably shorten T_1 and consequently increase MRI contrast leading to a brightening of T_1-weighted images (positive contrast agents).[121] Gd^{3+} ions have a high magnetic moment under a magnetic field due to their large number of unpaired electrons (seven) but are highly toxic. They are thus widely used as MRI contrast agents in the form of Gd^{3+} chelates, such as Gd-DTPA[122] or Gd-DOTA, to avoid cytotoxicity.

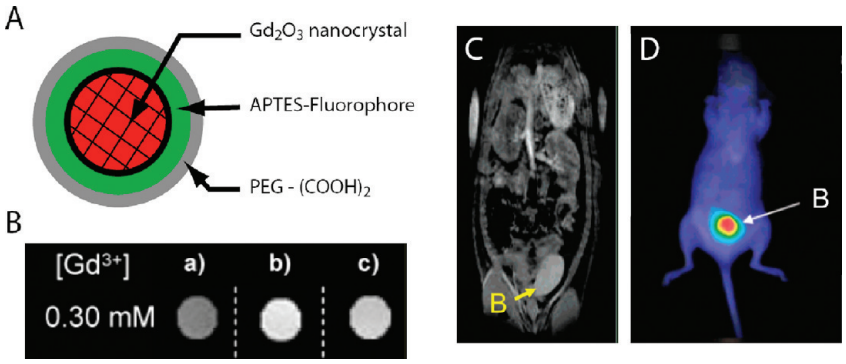

Figure 12. Bimodal MRI and fluorescence imaging using Gd_2O_3 nanoparticles. (A) Structure of the nanoparticles: The Gd_2O_3 core is coated by APTES containing a fluorophore and the nanoparticle is then covered by a PEG layer. (B) MRI images with (a) standard Gd-DOTA solution, (b) 2.2 nm nanoparticles, and (c) 3.8 nm nanoparticles. (C) MRI image of a living rat 1 h after nanoparticle injection. (D) Fluorescence image of a living rat. In both cases "B" indicates the bladder. Reprinted from ref 62. Copyright 2007 American Chemical Society.

Recently, gadolinium-based nanoparticles have been developed for MRI contrast enhancement[62−65] and multimodal imaging (MRI and fluorescence or X-ray)[62,123] or therapy by thermal neutron irradiation.[124] The use of nanoparticles leads to longer rotational correlation times which increase the proton relaxivity (defined as the modification of the inverse proton relaxation time due to the presence of the contrast agent over the contrast agent concentration) and, with an adequate coating, to longer blood circulation times. In addition, Gd^{3+}-ion leaching can be expected to be weaker when the ions are incorporated in solid nanoparticles rather than in a small organic molecule. Furthermore, nanoparticles can be used as a platform for grafting molecules allowing multimodal imaging and/or specific targeting *in vivo*.[125]

Gadolinium oxide nanoparticles (Gd_2O_3) were sequentially coated with aminopropyltriethoxy silane (APTES) coupled to a fluorophore and a polyethyleneglycol (PEG) layer to which biotargeting groups can be attached (Figure 12A). These nanoparticles enhance MRI contrast more efficiently than the Gd−DOTA complex, commonly used in clinical MRI, for the same concentration of Gd^{3+} ions (Figure 12B) and can also be imaged by fluorescence.[62] Notably, the effect of Gd^{3+} ions on water molecule relaxation still exists although they are covered by the PEG layer: This points to interesting possibilities of functionalization for biotargeting *in vivo*. Injection of Gd_2O_3 nanoparticles into a rat allows simultaneous MR and fluorescent imaging (Figure 12C,D) revealing its bladder.[62] Furthermore, $GdPO_4$ nanoparticles coated with dextran have been used for tumor detection, exploiting their long blood circulation time and the enhanced permeability and retention effect (EPR) of the tumor vasculature. Tumor visualization was possible with 1/10 of the dose typically used with Gd−DTPA.[65] An appropriate functionalization could enable the targeting of organ- or tumor-specific receptors,[126] opening new perspectives for medical imaging.

Gadolinium chelates were also used for the coating of gold nanoparticles to combine X-ray and MR imaging. The use of 2 nm Au@DTDTPA-Gd particles increases the contrast in both MRI and X-ray computed tomography (CT). Gold nanoparticles are indeed known to be good contrast agents for CT, and this effect is enhanced by the Gd-chelate coating. These nanoparticles are thus already good candidates for medical use.

The advantage of these hybrid nanoparticles compared to conventional techniques is notable: they combine in a single object the chemical properties required for different imaging modalities and for biotargeting.

CONCLUSION

The possibility to use rare-earth based nanoparticles has been demonstrated for many different biological applications, covering molecular and cell biology, *in vitro* and *in vivo* assays. They thus are an interesting alternative to existing methods. Their optical properties, photostability, absence of blinking, narrow or upconverted emission, large Stokes or anti-Stokes shifts, and long lifetime of excited states, and their absence of cytotoxicity make them suitable to replace organic dyes or quantum dots in all their reported applications. Their potentialities in living systems have been clearly established and applications leading to major biological breakthroughs are now appearing. The chemical properties of rare earth ions have thus allowed otherwise inaccessible measurements, like the dynamic detection of H_2O_2. In this case, rare-earth based nanoparticles are not only a convenient alternative to existing methods, but have revealed new biologically important information. Finally, one of the main advantages of rare-earth doped nanoparticles synthesized in water is their easy functionalization compared to quantum dots. Furthermore, combined properties for multiple imaging types can be obtained with a single particle. This facile combination of different modalities

and targeting molecules is likely to place rare-earth based nanoparticles as a central tool for biomedical imaging.

REFERENCES AND NOTES

1. Tsien, R. Y. Fluorescence Measurement and Photochemical Manipulation of Cytosolic Free Calcium. *Trends Neurosci.* **1988**, *11*, 419–424.
2. Cathcart, R.; Schwiers, E.; Ames, B. N. Detection of Picomole Levels of Hydroperoxides Using a Fluorescent Dichlorofluorescein Assay. *Anal. Biochem.* **1983**, *134*, 111–116.
3. Michalet, X.; Pinaud, F. F.; Bentolila, L. A.; Tsay, J. M.; Doose, S.; Li, J. J.; Sundaresan, G.; Wu, A. M.; Gambhir, S. S.; Weiss, S. Quantum Dots for Live Cells, *in Vivo* Imaging, and Diagnostics. *Science* **2005**, *307*, 538–544.
4. Medintz, I. L.; Uyeda, H. T.; Goldman, E. R.; Mattoussi, H. Quantum Dot Bioconjugates for Imaging, Labelling and Sensing. *Nat. Mater.* **2005**, *4*, 435–446.
5. Dahan, M.; Levi, S.; Luccardini, C.; Rostaing, P.; Riveau, B.; Triller, A. Diffusion Dynamics of Glycine Receptors Revealed by Single Quantum Dot Tracking. *Science* **2003**, *302*, 442–445.
6. Bouzigues, C.; Dahan, M. Transient Directed Motions of GABAA Receptors in Growth Cones Detected by a Speed Correlation Index. *Biophys. J.* **2007**, *92*, 654–60.
7. Dubertret, B.; Skourides, P.; Norris, D. J.; Noireaux, V.; Brivanlou, A. H.; Libchaber, A. In *Vivo* Imaging of Quantum Dots Encapsulated in Phospholipid Micelles. *Science* **2002**, *298*, 1759–1762.
8. Luccardini, C.; Tribet, C.; Vial, F.; Marchi-Artzner, V.; Dahan, M. Size, Charge, and Interactions with Giant Lipid Vesicles of Quantum Dots Coated with an Amphiphilic Macromolecule. *Langmuir* **2006**, *22*, 2304–10.
9. Faklaris, O.; Garrot, D.; Joshi, V.; Druon, F.; Boudou, J.-P.; Sauvage, T.; Georges, P.; Curmi, P. A.; Treussart, F. Detection of Single Photoluminescent Diamond Nanoparticles in Cells and Study of the Internalization Pathway. *Small* **2008**, *4*, 2236–39.
10. Chang, I. P.; Hwang, K. C.; Chiang, C. S. Preparation of Fluorescent Magnetic Nanodiamonds and Cellular Imaging. *J. Am. Chem. Soc.* **2008**, *130*, 15476–81.
11. Faklaris, O.; Joshi, V.; Irinopoulou, T.; Tauc, P.; Sennour, M.; Girard, H.; Gesset, C.; Arnault, J.-C.; Thorel, A.; Boudou, J.-P.; et al. Photoluminescent Diamond Nanoparticles for Cell Labeling: Study of the Uptake Mechanism in Mammalian Cells. *ACS Nano* **2009**, *3*, 3955–3962.
12. Santra, S.; Wang, K.; Tapec, R.; Tan, W. Development of Novel Dye-Doped Silica Nanoparticles for Biomarker Application. *J. Biomed. Opt.* **2001**, *6*, 160–166.
13. Ow, H.; Larson, D. R.; Srivastava, M.; Baird, B. A.; Webb, W. W.; Wiesner, U. Bright and Stable Core−Shell Fluorescent Silica Nanoparticles. *Nano Lett.* **2005**, *5*, 113–17.
14. Lasne, D.; Blab, G. A.; Berciaud, S.; Heine, M.; Groc, L.; Choquet, D.; Cognet, L.; Lounis, B. Single Nanoparticle Photothermal Tracking (SNaPT) of 5-nm Gold Beads in Live Cells. *Biophys. J.* **2006**, *91*, 4598–4604.
15. Klein, S.; Petersen, S.; Taylor, U.; Rath, D.; Barcikowski, S. Quantitative Visualization of Colloidal and Intracellular Gold Nanoparticles by Confocal Microscopy. *J. Biomed. Opt.* **2010**, *15*, 036015.
16. Shen, J.; Sun, L.-D.; Yan, C.-H. Luminescent Rare Earth Nanomaterials for Bioprobe Applications. *Dalton Trans.* **2008**, *14*, 5687–97.
17. Vetrone, F.; Capobianco, J. A. Lanthanide-Doped Fluoride Nanoparticles: Luminescence, Upconversion, and Biological Applications. *Int. J. Nanotechnol.* **2008**, *5*, 1306–1339.
18. Dosev, D.; Nichkova, M.; Kennedy, I. M. Inorganic Lanthanide Nanophosphors in Biotechnology. *J. Nanosci. Nanotechnol.* **2008**, *8*, 1052–1067.
19. Escribano, P.; Julian-Lopez, B.; Planelles-Arago, J.; Cordoncillo, E.; Viana, B.; Sanchez, C. Photonic and Nanobiophotonic Properties of Luminescent Lanthanide-Doped Hybrid Organic−Inorganic Materials. *J. Mater. Chem.* **2008**, *18*, 23–40.
20. Petoud, S.; Cohen, S. M.; Bunzli, J. C. G.; Raymond, K. N. Stable Lanthanide Luminescence Agents Highly Emissive in Aqueous Solution: Multidentate 2-Hydroxyisophthalamide Complexes of Sm^{3+}, Eu^{3+}, Tb^{3+}, Dy^{3+}. *J. Am. Chem. Soc.* **2003**, *125*, 13324–13325.
21. Selvin, P. R. Principles and Biophysical Applications of Lanthanide-Based Probes. *Annu. Rev. Biophys. Biomol. Struct.* **2002**, *31*, 275–302.
22. Charbonniere, L. J.; Hildebrandt, N. Z., R.F.; Loehmannsroeben, H. G. Lanthanides to Quantum Dots Resonance Energy Transfer in Time-Resolved Fluoro-Immunoassays and Luminescence Microscopy. *J. Am. Chem. Soc.* **2006**, *128*, 12800–12809.
23. Pellegatti, L.; Zhang, J.; Drahos, B.; Villette, S.; Suzenet, F.; Guillaument, G.; Petoud, S.; Toth, E. Pyridine-Based Lanthanide Complexes: Towards Bimodal Agents Operating as near Infrared Luminescent and MRI Reporters. *Chem. Commun.* **2008**, *48*, 6591–6593.
24. Riwotzki, K.; Haase, M. Colloidal YVO_4: Eu and $YP_{0.95}V_{0.05}O_4$: Eu Nanoparticles: Luminescence and Energy Transfer Processes. *J. Phys. Chem. B* **1998**, *105*, 12709–12713.
25. Huignard, A.; Gacoin, T.; Boilot, J.-P. Synthesis and Luminescence Properties of Colloidal YVO4:Eu Phosphors. *Chem. Mater.* **2000**, *12*, 1090–1094.
26. Blasse, G.; Grabmeier, B. C., *Luminescent Materials*; Springer-Verlag: Berlin, 1994.
27. Amans, D.; Malaterre, C.; Diouf, M.; Mancini, C.; Chaput, F.; Ledoux, G.; Breton, G.; Guillin, Y.; Dujardin, C.; Masenelli-Varlot, K.; et al. Synthesis of Oxide Nanoparticles by Pulsed Laser Ablation in Liquids Containing a Complexing Molecule: Impact on Size Distributions and Prepared Phases. *J. Phys. Chem. C* **2011**, *115*, 5131–5139.
28. Williams, D. K.; Yuan, H.; Tissue, B. M. Size Dependence of the Luminescence Spectra and Dynamics of Eu^{3+}: Y_2O_3 Nanocrystals. *J. Lumin.* **1999**, *83−4*, 297–300.
29. Meyssamy, H.; Riwotzki, K.; Kornowski, A.; Naused, S.; Haase, M. Wet-chemical Synthesis of Doped Colloidal Nanomaterials: Particles and Fibers of $LaPO_4$:Eu, $LaPO_4$: Ce, and $LaPO_4$:Ce,Tb. *Adv. Mater.* **1999**, *11*, 840.
30. Huignard, A.; Buissette, V.; Laurent, G.; Gacoin, T.; Boilot, J.-P. Synthesis and Characterizations of YVO4:Eu Colloids. *Chem. Mater.* **2002**, *14*, 2264–2269.
31. Feng, W.; Sun, L.-D.; Zhang, Y.-W.; Yan, C.-H. Synthesis and Assembly of Rare Earth Nanostructures Directed by the Principle of Coordination Chemistry in Solution-Based Process. *Coord. Chem. Rev.* **2010**, *254*, 1038–1053.
32. Beaurepaire, E.; Buissette, V.; Sauviat, M.-P.; Giaume, D.; Lahlil, K.; Mercuri, A.; Casanova, D.; Huignard, A.; Martin, J.-L.; Gacoin, T.; et al. Functionalized Fluorescent Oxide Nanoparticles: Artificial Toxins for Sodium Channel Targeting and Imaging at the Single-Molecule Level. *Nano Lett.* **2004**, *4*, 2079–2083.
33. Son, A.; Dosev, D.; Nichkova, M.; Ma, Z.; Kennedy, I. M.; Scow, K. M.; Hristova, K. R. Quantitative DNA Hybridization in Solution Using Magnetic/Luminescent Core−Shell Nanoparticles. *Anal. Biochem.* **2007**, *370*, 186–194.
34. Wang, L.; Li, P.; Wang, L. Luminescent and Hydrophilic LaF_3-Polymer Nanocomposite for DNA Detection. *Luminescence* **2008**, *24*, 39–44.
35. Hirai, T.; Orikoshi, T.; Komasawa, I. Preparation of Y_2O_3: Yb,Er Infrared-to-Visible Conversion Phosphor Fine Particles Using an Emulsion Liquid Membrane System. *Chem. Mater.* **2002**, *14*, 3576–3583.
36. van de Rijke, F.; Zijlmans, H.; Li, S.; Vail, T.; Raap, A. K.; Niedbala, R. S.; Tanke, H. J. Up-Converting Phosphor Reporters for Nucleic Acid Microarrays. *Nat. Biotechnol.* **2001**, *19*, 273–276.
37. Yi, G.; Sun, B.; Yang, F.; Chen, D.; Zhou, Y.; Cheng, J. Synthesis and Characterization of High-Efficiency Nanocrystal Up-Conversion Phosphors: Ytterbium and Erbium Codoped Lanthanum Molybdate. *Chem. Mater.* **2002**, *14*, 2910–2914.

38. Yi, G.; Lu, H.; Zhao, S.; Ge, Y.; Yang, W.; Chen, D.; Guo, L.-H. Synthesis, Characterization, and Biological Application of Size-Controlled Nanocrystalline NaYF4:Yb,Er Infrared-to-Visible Up-Conversion Phosphors. *Nano Lett.* **2004**, *4*, 2191–2196.
39. Kobayashi, H.; Kosaka, N.; Ogawa, M.; Morgan, N. Y.; Smith, P. D.; Murray, C. B.; Ye, X.; Collins, J.; Kumar, G. A.; Bell, H.; et al. *In Vivo* Multiple Color Lymphatic Imaging Using Upconverting Nanocrystals. *J. Mater. Chem.* **2009**, *19*, 6481–6484.
40. Wu, S.; Han, G.; Milliron, D. J.; Aloni, S.; Altoe, V.; Talapin, D. V.; Cohen, B. E.; Schuck, P. J. Nonblinking and Photostable Upconverted Luminescence from Single Lanthanide-Doped Nanocrystals. *Proc. Natl. Acad. Sci. U.S.A.* **2009**, *106*, 10917–10921.
41. Mialon, G.; Turkcan, S.; Alexandrou, A.; Gacoin, T.; Boilot, J.-P. New Insights into Size Effects in Luminescent Oxide Nanocrystals. *J. Phys. Chem. C* **2009**, *113*, 18699–18706.
42. le Masne de Chermont, Q.; Chanéac, C.; Seguin, J.; Pellé, F.; Maîtrejean, S.; Jolivet, J.-P.; Gourier, D.; Bessodes, M.; Scherman, D. Nanoprobes with Near-Infrared Persistent Luminescence for *in Vivo* Imaging. *Proc. Natl. Acad. Sci. U.S.A.* **2007**, *104*, 9266–9271.
43. Lehmann, O.; Kompe, K.; Haase, M. Synthesis of Eu^{3+}-doped Core and Core/Shell Nanoparticles and Direct Spectroscopic Identification of Dopant Sites at the Surface and in the Interior of the Particles. *J. Am. Chem. Soc.* **2004**, *126*, 14935–14942.
44. Murray, K.; Cao, Y.-C.; Ali, S.; Hanley, Q. Lanthanide Doped Silicananoparticles Applied to Multiplexed Immunoassays. *Analyst* **2010**, *135*, 2132–2138.
45. Shao, Y. Z.; Liu, L. Z.; Song, S. Q.; Cao, R. H.; Liu, H.; Cui, C. Y.; Li, X.; Bie, M. J.; Li, L. A Novel One-Step Synthesis of Gd^{3+}-Incorporated Mesoporous SiO_2 Nanoparticles for Use as an Efficient MRI Contrast Agent. *Contrast Media Mol. Imaging* **2011**, *6*, 110–118.
46. Soukka, T.; Härmä, H. Lanthanide Nanoparticules as Photoluminescent Reporters. *Springer Ser. Fluoresc.* **2011**, *7*, 89–113.
47. Yang, J.; Aschemeyer, S.; Kummel, A. C.; Trogler, W. C.; Sandoval, S.; Liberman, A.; Alfaro, J.; Martin, D. T.; Makale, M. T. Red-Luminescent Europium (III) Doped Silica Nanoshells: Synthesis, Characterization, and Their Interaction with HeLa Cells. *J. Biomed. Opt.* **2011**, *16*, 066012.
48. Ma, Z. Y.; Dosev, D.; Kennedy, I. M. A Microemulsion Preparation of Nanoparticles of Europium in Silica with Luminescence Enhancement Using Silver. *Nanotechnology* **2009**, *20*, 085608.
49. Xie, C. N.; Yang, Z. M.; Sun, Y. H. Synthesis and Characterization of Monodispersed SiO_2@$Y_3Al_5O_{12}$:Er^{3+} Core−Shell Particles. *J. Fluoresc.* **2009**, *19*, 623–629.
50. Xu, Y.; Li, Q. Multiple Fluorescent Labeling of Silica Nanoparticles with Lanthanide Chelates for Highly Sensitive Time-Resolved Immunofluorometric Assays. *Clin. Chem.* **2007**, *53*, 1503–10.
51. Samuel, J.; Tallec, G.; Cherns, P.; Ling, W. L.; Raccurt, O.; Poncelet, O.; Imbert, D.; Mazzanti, M. Lanthanide-Chelate Silica Nanospheres as Robust Multicolor Vis-NIR Tags. *Chem. Commun.* **2010**, *46*, 2647–9.
52. Huhtinen, P.; Kivelä, M.; Kuronen, O.; Hagren, V.; Takalo, H.; Tenhu, H.; Lövgren, T.; Härmä, H. Synthesis, Characterization, and Application of Eu(III), Tb(III), Sm(III), and Dy(III) Lanthanide Chelate Nanoparticle Labels. *Anal. Chem.* **2005**, *77*, 2643–8.
53. Huhtinen, P.; Kivelä, M.; Soukka, T.; Tenhu, H.; Lövgren, T.; Härmä, H. Preparation, Characterisation and Application of Europium(III) Chelate-Dyed Polystyrene-Acrylic Acid Nanoparticle Labels. *Anal. Chim. Acta* **2008**, *630*, 211–6.
54. Näreoja, T.; Vehniäinen, M.; Lamminmäki, U.; Hänninen, P. E.; Härmä, H. Study on Nonspecificity of an Immuoassay Using Eu-Doped Polystyrene Nanoparticle Labels. *J. Immunol. Methods* **2009**, *345*, 80–89.
55. Basiruddin, S. K.; Saha, A.; Pradhan, N.; Jana, N. R. Advances in Coating Chemistry in Deriving Soluble Functional Nanoparticle. *J. Phys. Chem. C* **2010**, *114*, 11009–11017.
56. Casanova, D.; Giaume, D.; Moreau, M.; Martin, J.-L.; Gacoin, T.; Boilot, J.-P.; Alexandrou, A. Counting the Number of Proteins Coupled to Single Nanoparticles. *J. Am. Chem. Soc.* **2007**, *129*, 12592–12593.
57. Giaume, D.; Poggi, M.; Casanova, D.; Mialon, G.; Lahlil, K.; Alexandrou, A.; Gacoin, T.; Boilot, J.-P. Organic Functionalization of Luminescent Oxide Nanoparticles toward their Application as Biological Probes. *Langmuir* **2008**, *24*, 11018–11026.
58. Johnson, N. J.; Sangeetha, N. M.; Boyer, J. C.; van Veggel, F. C. Facile Ligand-Exchange with Polyvinylpyrrolidone and Subsequent Silica Coating of Hydrophobic Upconverting Beta-$NaYF_4$:Yb^{3+}/Er^{3+} Nanoparticles. *Nanoscale* **2010**, *2*, 771–777.
59. Dong, A.; Ye, X.; Chen, J.; Kang, Y.; Gordon, T.; Kikkawa, J. M.; Murray, C. B. A Generalized Ligand-Exchange Strategy Enabling Sequential Surface Functionalization of Colloidal Nanocrystals. *J. Am. Chem. Soc.* **2011**, *133*, 998–1006.
60. Safi, M.; Sarrouj, H.; Sandre, O.; Mignet, N.; Berret, J.-F. Interactions between Sub-10-nm Iron and Cerium Oxide Nanoparticles and 3T3 Fibroblasts: The Role of the Coating and Aggregation State. *Nanotechnology* **2010**, *21*, 145103.
61. Mornet, S.; Vasseur, S.; Grasset, F.; Duguet, E. Magnetic Nanoparticle Design for Medical Diagnosis and Therapy. *J. Mater. Chem.* **2004**, *14*, 2161–2175.
62. Bridot, J.-L.; Faure, A.-C.; Laurent, S.; Rivière, C.; Billotey, C.; Hiba, B.; Janier, M.; Josserand, V.; Coll, J.-L.; Van der Elst, L.; et al. Hybrid Gadolinium Oxide Nanoparticles: Multimodal Contrast Agents for *in Vivo* Imaging. *J. Am. Chem. Soc.* **2007**, *129*, 5076–5084.
63. Park, Y. I.; Kim, J. H.; Lee, K. T.; Jeon, K.-S.; Na, H. B.; Yu, J. H.; Kim, H. M.; Lee, N.; Choi, S. H.; Baik, S.-I.; et al. Nonblinking and Nonbleaching Upconverting Nanoparticles as an Optical Imaging Nanoprobe and T_1 Magnetic Resonance Imaging Contrast. *Adv. Mater.* **2009**, *21*, 4467–4471.
64. Hifumi, H.; Yamaoka, S.; Tanimoto, A.; Citterio, D.; Suzuki, K. Gadolinium-Based Hybrid Nanoparticles as a Positive MR Contrast Agent. *J. Am. Chem. Soc.* **2006**, *128*, 15090–15091.
65. Hifumi, H.; Yamaoka, S.; Tanimoto, A.; Akatsu, T.; Shindo, Y.; Honda, A.; Citterio, D.; Oka, K.; Kuribayashi, S.; Suzuki, K. Dextran Coated Gadolinium Phosphate Nanoparticles for Magnetic Resonance Tumor Imaging. *J. Mater. Chem.* **2009**, *19*, 6393–6399.
66. Li, Y. L.; Jiang, H. L.; Ni, T. Y.; Zhang, T. Y.; Tao, Z. H.; Zeng, Y. H. Diode-Pumped Nd:YVO_4/Nd:YLF Laser at 488 nm. *Laser Phys.* **2011**, *21*, 677–679.
67. Wright, J. C. Up-Conversion and Excited State Energy Transfer in Rare-Earth Doped Materials. *Top. Appl. Phys.* **1976**, *15*, 239–295.
68. Heer, S.; Lehmann, O.; Haase, M.; Güdel, H.-U. Blue, Green, and Red Upconversion Emission from Lanthanide-Doped $LuPO_4$ and $YbPO_4$ Nanocrystals in a Transparent Colloidal Solution. *Angew. Chem., Int. Ed.* **2002**, *42*, 3179–3182.
69. Mialon, G.; Türkcan, S.; Dantelle, G.; Collins, D. P.; Hadjipanayi, M.; Taylor, R. A.; Gacoin, T.; Alexandrou, A.; Boilot, J.-P. High Up-Conversion Efficiency of YVO4:Yb, Er Nanoparticles in Water down to the Single-Particle Level. *J. Phys. Chem. C* **2010**, *114*, 22449–22454.
70. Casanova, D.; Giaume, D.; Gacoin, T.; Boilot, J.-P.; Alexandrou, A. Optical *in Situ* Size Determination of Single Lanthanide-Ion Doped Oxide Nanoparticles. *Appl. Phys. Lett.* **2006**, *89*, 253103.
71. Casanova, D.; Giaume, D.; Gacoin, T.; Boilot, J.-P.; Alexandrou, A. Single Lanthanide-Doped Oxide Nanoparticles as Donors in Fluorescence Resonance Energy Transfer. *J. Phys. Chem. B* **2006**, *110*, 19264–19270.
72. Mialon, G.; Poggi, M.; Casanova, D.; Nguyen, T.-L.; Turckan, S.; Alexandrou, A.; Gacoin, T.; Boilot, J.-P. Luminescent Oxide Nanoparticles with Enhanced Optical Properties. *J. Lumin.* **2009**, *129*, 1706–1710.
73. Mialon, G.; Gohin, M.; Gacoin, T.; Boilot, J.-P. High Temperature Strategy for Oxide Nanoparticle Synthesis. *ACS Nano* **2008**, *2*, 2505–12.

74. Wang, H.-Q.; Nann, T. Monodisperse Upconverting Nanocrystals by Microwave-Assisted Synthesis. *ACS Nano* **2009**, *3*, 3804–3808.
75. Dosev, D.; Nichkova, M.; Liu, M.; Guo, B.; Liu, G. Y.; Hammock, B. D.; Kennedy, I. M. Application of Luminescent Eu:Gd_2O_3 Nanoparticles to the Visualization of Protein Micropatterns. *J. Biomed. Opt.* **2005**, *10*, 064006.
76. Idris, N. M.; Li, Z.; Ye, L.; Sim, E. K. W.; Mahendran, R.; Ho, P. C.-L.; Zhang, Y. Tracking Transplanted Cells in Live Animal Using Upconversion Fluorescent Nanoparticles. *Biomaterials* **2009**, *30*, 5104–5113.
77. Casanova, D.; Bouzigues, C.; Nguyên, T. L.; Ramodiharilafy, R. O.; Bouzhir-Sima, L.; Gacoin, T.; Boilot, J.-P.; Tharaux, P.-L.; Alexandrou, A. Single Europium-Doped Nanoparticles Measure Temporal Pattern of Reactive Oxygen Species Procuction inside Cells. *Nat. Nanotechnol.* **2009**, *4*, 581–585.
78. Mahler, B.; Spinicelli, P.; Buil, S.; Quelin, X.; Hermier, J.-P.; Dubertret, B. Towards Nonblinking Colloidal Quantum Dots. *Nat. Mater.* **2008**, *7*, 659–664.
79. Wang, X.; Ren, X.; Kahen, K.; Hahn, M. A.; Rajeswaran, M.; Maccagnano-Zacher, S.; Silcox, J.; Cragg, G. E.; Efros, A. L.; Krauss, T. D. Nonblinking Semiconductor Nanocrystals. *Nature* **2009**, *459*, 686–689.
80. Türkcan, S.; Casanova, D.; Masson, J.-B.; Mialon, G.; Popoff, M. R.; Gacoin, T.; Boilot, J.-P.; Alexandrou, A. Observing the Confinement Potential of Bacterial Pore-Forming Toxin Receptors with Nonblinking Eu^{3+}-doped Oxide Nanoparticles. Unpublished work.
81. Dabbousi, B. O.; Rodriguez-Viejo, J.; Mikulec, F. V.; Heine, J. R.; Matoussi, H.; Ober, R.; Jensen, K. F.; Bawendi, M. G. (CdSe)ZnS Core−Shell Quantum Dots: Synthesis and Characterization of a Size Series of Highly Luminescent Nanocrystallites. *J. Phys. Chem. B* **1997**, *101*, 9463–9475.
82. Leatherdale, C. A.; Woo, W.-K.; Mikulec, F. V.; Bawendi, M. G. On the Absorption Cross Section of CdSe Nanocrystal Quantum Dots. *J. Phys. Chem. B* **2002**, *106*, 7619–7622.
83. Grabolle, M.; Ziegler, J.; Merkulov, A.; Nann, T.; Resch-Genger, U. Stability and Fluorescence Quantum Yield of CdSe−ZnS Quantum Dots: Influence of the Thickness of the ZnS Shell. *Ann. N.Y. Acad. Sci.* **2008**, *1130*, 235–241.
84. Dahan, M.; Laurence, T.; Pinaud, F.; Chemla, D. S.; Alivisatos, P.; Sauer, M.; Weiss, S. Time-Gated Biological Imaging by Use of Colloidal Quantum Dots. *Opt. Lett.* **2001**, *26*, 825–827.
85. Wee, T. S.; Tzeng, Y. K.; Han, C. C.; Chang, H. C.; Fann, W.; Hsu, J. H.; Chen, K. M.; Yu, Y. C. Two-Photon Excited Fluorescence of Nitrogen-Vacancy Centers in Proton-Irradiated Type Ib Diamond. *J. Phys. Chem. A* **2007**, *111*, 9379–9386.
86. Davies, G. *Properties and Growth of Diamond*; INSPEC, The Institution of Electrical Engineers: London, 1994.
87. Jamieson, T.; Bakhshi, R.; Petrova, D.; Pocock, R.; Imani, M.; Seifalian, A. M. Biological Applications of Quantum Dots. *Biomaterials* **2007**, *28*, 4717–4732.
88. Bottrill, M.; Green, M. Some Aspects of Quantum Dot Toxicity. *Chem. Commun.* **2011**, *47*, 7039–7050.
89. Nyk, M.; Kumar, R.; Ohulchanskyy, T. Y.; Bergey, E. J.; Prasad, P. N. High Contrast *in Vitro* and *in Vivo* Photoluminescence Bioimaging Using near Infrared to near Infrared Up-conversion in Tm^{3+} and Yb^{3+} Doped Fluoride Nanophosphors. *Nano Lett.* **2008**, *8*, 3834–3838.
90. Lewinski, N.; Colvin, V.; Drezek, R. Cytotoxicity of Nanoparticles. *Small* **2008**, *4*, 26–49.
91. Son, A.; Nichkova, M.; Dosev, D.; Kennedy, I. M.; Hristova, K. R. Luminescent Lanthanide Nanoparticles as Labels in DNA Microarrays for Quantification of Methyl Tertiary Butyl Ether Degrading Bacteria. *J. Nanosci. Nanotechnol.* **2008**, *8*, 2463–2467.
92. Son, A.; Dhirapong, A.; Dosev, D. K.; Kennedy, I. M.; Weiss, R. H.; Hristova, K. R. Rapid and Quantitative DNA Analysis of Genetic Mutations for Polycystic Kidney Disease (PKD) Using Magnetic/Luminescent Nanoparticles. *Anal. Bioanal. Chem.* **2008**, *390*, 1829–1835.
93. Ogata, A.; Tagoh, H.; Lee, T.; Kuritani, T.; Takahara, Y.; Shimamura, T.; Ikegami, H.; Kurimoto, M.; Yoshizaki, K.; Kishimoto, T. A New Highly Sensitive Immunoassay for Cytokines by Dissociation-Enhanced Lanthanide Fluoroimmunoassay (DELFIA). *J. Immunol. Methods* **1992**, *148*, 15–22.
94. Moore, E. G.; Samuel, A. P.; Raymond, K. N. From Antenna to Assay: Lessons Learned in Lanthanide Luminescence. *Acc. Chem. Res.* **2009**, *42*, 542–552.
95. Sapsford, K. E.; L., B.; Medintz, I. L. Materials for Fluorescence Resonance Energy Transfer Analysis: Beyond Traditional Donor−Acceptor Combinations. *Angew. Chem., Int. Ed.* **2006**, *45*, 4562–4589.
96. Mathis, G. HTRF(R) Technology. *J. Biomol. Screen.* **1999**, *4*, 309–313.
97. Cummings, R. T.; McGovern, H. M.; Zheng, S.; Park, Y. W.; Hermes, J. D. Use of a Phosphotyrosine-Antibody Pair as a General Detection Method in Homogeneous Time-Resolved Fluorescence: Application to Human Immunodeficiency Viral Protease. *Anal. Biochem.* **1999**, *10*, 79–93.
98. Ghose, S.; Trinquet, E.; Laget, M.; Bazin, H.; Mathis, G. Rare Earth Cryptates for the Investigation of Molecular Interactions *in Vitro* and in Living Cells. *J. All. Comp.* **2008**, *451*, 35–37.
99. Härmä, H.; Dähne, L.; Pihlasalo, S.; Suojanen, J.; Peltonen, J.; Hänninen, P. Sensitive Quantitative Protein Concentration Method Using Luminescent Resonance Energy Transfer on a Layer-by-Layer Europium(III) Chelate Particle Sensor. *Anal. Chem.* **2008**, *80*, 9781–9786.
100. Pihlasalo, S.; Pellonperä, L.; Martikkala, E.; Hänninen, P. E.; Härmä, H. Sensitive Fluorometric Nanoparticle Assays for Cell Counting and Viability. *Anal. Chem.* **2010**, *82*, 9282–8.
101. Kuningas, K.; Rantanen, T.; Ukonaho, T.; Lövgren, T.; Soukka, T. Homogeneous Assay Technology Based on Upconverting Phosphors. *Anal. Chem.* **2005**, *77*, 7348–7355.
102. Vetrone, F.; Naccache, R.; Morgan, C. G.; Capobianco, J. A. Luminescence Resonance Energy Transfer from an Upconverting Nanoparticle to a Fluorescent Phycobiliprotein. *Nanoscale* **2010**, *2*, 1185–9.
103. Kuningas, K.; Ukonaho, T.; Päkkilä, H.; Rantanen, T.; Rosenberg, J.; Lövgren, T.; Soukka, T. Upconversion Fluorescence Resonance Energy Transfer in a Homogeneous Immunoassay for Estradiol. *Anal. Biochem.* **2006**, *78*, 4690–4696.
104. Kuningas, K.; Päkkilä, H.; Ukonaho, T.; Rantanen, T.; Lövgren, T.; Soukka, T. Upconversion Fluorescence Enables Homogeneous Immunoassay in Whole Blood. *Clin. Chem.* **2007**, *53*, 145–146.
105. Rantanen, T.; Järvenpää, M. L.; Vuojola, J.; Kuningas, K.; Soukka, T. Fluorescence-Quenching-Based Enzyme-Activity Assay by Using Photon Upconversion. *Angew. Chem., Int. Ed.* **2008**, *47*, 3811–3813.
106. Soukka, T.; Rantanen, T.; Kuningas, K. Photon Upconversion in Homogeneous Fluorescence-Based Bioanalytical Assays. *Ann. N.Y. Acad. Sci.* **2008**, *1130*, 188–200.
107. Lim, S. F.; Riehn, R.; Ryu, W. S.; Khanarian, N.; Tung, C.-K.; Tank, D.; Austin, R. H. *In Vivo* and Scanning Electron Microscopy Imaging of Upconverting Nanophosphors in Caenorhabditis Elegans. *Nano Lett.* **2006**, *6*, 169–174.
108. Yu, M.; Li, F.; Chen, Z.; Hu, H.; Zhan, C.; Yang, H.; Huang, C. Laser Scanning Up-Conversion Luminescence Microscopy for Imaging Cells Labeled with Rare-Earth Nanophosphors. *Anal. Chem.* **2009**, *81*, 930–935.
109. Hille, B. The Receptor for Tetrodotoxin and Saxitoxin. A Structural Hypothesis. *Biophys. J.* **1975**, *15*, 615–619.
110. Courty, S.; Luccardini, C.; Cappello, G.; Bellaiche, Y.; Dahan, M. Tracking Individual Kinesin Motors in Living Cells Using Single Quantum Dot Imaging. *Nano Lett.* **2006**, *6*, 1491–5.
111. Gautier, A.; Juillerat, A.; Heinis, C.; Corrêa, I. R. J.; Kindermann, M.; Beaufils, F.; Johnsson, K. An Engineered Protein Tag for Multiprotein Labeling in Living Cells. *Chem. Biol.* **2008**, *15*, 128–36.
112. Ruenraroengsak, P.; Al-Jamal, K. T.; Hartell, N.; Braeckmans, K.; De Smedt, S. C.; Florence, A. T. Cell Uptake, Cytoplasmic

Diffusion and Nuclear Access of a 6.5 nm Diameter Dendrimer. *Int. J. Pharm.* **2007**, *331*, 215–219.
113. Kusumi, A.; Sako, Y.; Yamamoto, M. Confined Lateral Diffusion of Membrane Receptors as Studied by Single Particle Tracking (Nanovid Microscopy). Effects of Calcium-Induced Differentiation in Cultured Epithelial Cells. *Biophys. J.* **1993**, *65*, 2021–2040.
114. Choquet, D.; Triller, A. The Role of Receptor Diffusion in the Organization of the Postsynaptic Membrane. *Nat. Rev. Neurosci.* **2003**, *4*, 251–265.
115. Lommerse, P. H.; Blab, G. A.; Cognet, L.; Harms, G. S.; Snaar-Jagalska, B. E.; Spaink, H. P.; Schmidt, T. Single-Molecule Imaging of the H-ras Membrane-Anchor Reveals Domains in the Cytoplasmic Leaflet of the Cell Membrane. *Biophys. J.* **2004**, *86*, 609–616.
116. Bonneau, S.; Cohen, L.; Dahan, M. Single Quantum Dot Tracking Based on Perceptual Grouping Using Minimal Paths in a Spatio-Temporal Volume. *IEEE Trans. Image Process.* **2004**, *14*, 1384–1395.
117. Bouzigues, C.; Morel, M.; Triller, A.; Dahan, M. Asymmetric Redistribution of GABA Receptors during GABA Gradient Sensing by Nerve Growth Cones Analyzed by Single Quantum Dot Imaging. *Proc. Natl. Acad. Sci. U.S.A.* **2007**, *104*, 11251–11256.
118. Masson, J.-B.; Casanova, D.; Türckan, S.; Voisinne, G.; Popoff, M. R.; Vergassola, M.; Alexandrou, A. Inferring Maps for Forces inside Cell Membrane Microdomains. *Phys. Rev. Lett.* **2009**, *102*, 048103.
119. Belousov, V. V.; Fradkov, A. F.; Lukyanov, K. A.; Staroverov, D. B.; Shakhbazov, D. B.; Shakhbazov, K. S.; Terskikh, A. V.; Lukyanov, S. Genetically Encoded Fluorescent Indicator for Intracellular Hydrogen Peroxide. *Nat. Methods* **2008**, *3*, 281–286.
120. Laurent, S.; Bridot, J.-L.; Elst, L. V.; Muller, R. N. Magnetic Iron Oxide Nanoparticles for Biomedical Applications. *Future Med. Chem.* **2010**, *2*, 427–449.
121. Bottrill, M.; Kwok, L.; Long, N. J. Lanthanides in Magnetic Resonance Imaging. *Chem. Soc. Rev.* **2006**, *35*, 557–571.
122. Carr, D. H.; Brown, J.; Bydder, G. M.; Steiner, R. E.; Weinmann, H.-J.; Speck, U.; Hall, A. S.; Young, I. R. Gadolinium−DTPA as a Contrast Agent in MRI: Initial Clinical Experience in 20 patients. *Am. J. Roentgenol.* **1984**, *143*, 215–224.
123. Alric, C.; Taleb, J.; Le Duc, G.; Mandon, C.; Billotey, C.; Le Meur-Herland, A.; Brochard, T.; Vocanson, F.; Janier, M.; Perriat, P.; et al. Gadolinium Chelate Coated Gold Nanoparticles as Contrast Agents for both X-ray Computed Tomography and Magnetic Resonance Imaging. *J. Am. Chem. Soc.* **2008**, *130*, 5908–15.
124. Bridot, J.-L.; Dayde, D.; Rivière, C.; Mandon, C.; Billotey, C.; Lerondel, S.; Sabattier, R.; Cartron, G.; Le Pape, A.; Blondiaux, G. O.; et al. Hybrid Gadolinium Oxide Nanoparticles Combining Imaging and Therapy. *J. Mater. Chem.* **2009**, *19*, 2328–2335.
125. Lewin, M.; Carlesso, N.; Tung, C. H.; Tang, X. W.; Cory, D.; Scadden, D. T.; Weissleder, R. Tat Peptide-derivatized Magnetic Nanoparticles Allow *in Vivo* Tracking and Recovery of Progenitor Cells. *Nat. Biotechnol.* **2000**, *18*, 410–414.
126. Islam, T.; Josephson, L. Current State and Future Applications of Active Targeting in Malignancies Using Superparamagnetic Iron Oxide Nanoparticles. *Cancer Biomark.* **2009**, *5*, 99–107.